Clay Generic Disposal System Model – Sensitivity Analysis for 32 PWR Assembly Canisters

Fuel Cycle Research & Development

Revision History

Version/Date	Description
27Sept2013	Submitted by Mark Nutt/ANL as FCRD-UFD-2013-000390
13Oct2014	Reviewed and approved at Sandia for Unclassified Unlimited Release (SAND2014-****)

Approved for Unclassified, Unlimited Release

Note: This document is paginated for screen viewing.

Sandia National Laboratories

Appendix E
FCT Document Cover Sheet

Name/Title of Deliverable/Milestone/ Revision No.	Clay Generic Disposal System Model – Sensitivity Analysis for 32 PWR Assembly Canisters
Work Package Title and Number	Generic Disposal System Level Modeling – ANL / FT-13-AN080801
Work Package WBS Number	1.02.08.08
Responsible Work Package Manager	W.Mark Nutt _(signature)_
	(Name/Signature)

Date Submitted _____

Quality Rigor Level for Deliverable/Milestone	☒ QRL-3	☐ QRL-2	☐ QRL-1 ☐ Nuclear Data	☐ Lab Participant QA Program (no additional FCT QA requirements)

This deliverable was prepared in accordance with   Argonne National Laboratory
                                                                                           (Participant/National Laboratory Name)

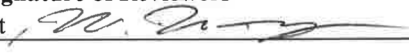QA program which meets the requirements of
         ☒ DOE Order 414.1   ☐ NQA-1-2000   ☐ Other

This Deliverable was subjected to:

☒ Technical Review	☐ Peer Review
Technical Review (TR)	**Peer Review (PR)**
Review Documentation Provided	**Review Documentation Provided**
☐ Signed TR Report or,	☐ Signed PR Report or,
☐ Signed TR Concurrence Sheet or,	☐ Signed PR Concurrence Sheet or,
☐ Signature of TR Reviewer(s) below	☐ Signature of PR Reviewer(s) below

Name and Signature of Reviewers

W. Mark Nutt _(signature)_

NOTE 1: *Appendix E should be filled out and submitted with the deliverable. Or, if the PICS:NE system permits, completely enter all applicable information in the PICS:NE Deliverable Form. The requirement is to ensure that all applicable information is entered either in the PICS:NE system or by using the FCT Document Cover Sheet.*

NOTE 2: *In some cases there may be a milestone where an item is being fabricated, maintenance is being performed on a facility, or a document is being issued through a formal document control process where it specifically calls out a formal review of the document. In these cases, documentation (e.g., inspection report, maintenance request, work planning package documentation or the documented review of the issued document through the document control process) of the completion of the activity, along with the Document Cover Sheet, is sufficient to demonstrate achieving the milestone. If QRL 1, 2, or 3 is not assigned, then the Lab / Participant QA Program (no additional FCT QA requirements) box must be checked, and the work is understood to be performed and any deliverable developed in conformance with the respective National Laboratory / Participant, DOE or NNSA-approved QA Program.*

CONTENTS

FIGURES

TABLES

USED FUEL DISPOSITION CAMPAIGN

CLAY GENERIC DISPOSAL SYSTEM MODEL – SENSITIVITY ANALYSIS FOR 32 PWR ASSEMBLY CANISTERS

1. INTRODUCTION

The Used Fuel Disposition Campaign (UFDC), as part of the DOE Office of Nuclear Energy's (DOE-NE) Fuel Cycle Technology program (FCT) is investigating the disposal of high level radioactive waste (HLW) and spent nuclear fuel[a] (SNF) in a variety of geologic media. The feasibility of disposing SNF and HLW in clay media has been investigated and has been shown to be promising [Ref. 1]. In addition the disposal of these wastes in clay media is being investigated in Belgium, France, and Switzerland. Thus, Argillaceous media is one of the environments being considered by UFDC. As identified by researchers at Sandia National Laboratory, potentially suitable formations that may exist in the U.S. include mudstone, clay, shale, and argillite formations [Ref. 1]. These formations encompass a broad range of material properties. In this report, reference to clay media is intended to cover the full range of material properties.

This report presents the status of the development of a simulation model for evaluating the performance of generic clay media. The clay Generic Disposal System Model (GDSM) repository performance simulation tool has been developed with the flexibility to evaluate not only different properties, but different waste streams/forms and different repository designs and engineered barrier configurations/ materials that could be used to dispose of these wastes.

In a previous report [Ref. 2] the clay GDSM simulation tool was described and was verified by comparing results with an analytical solution to the diffusion equation and by comparing calculations with results reported for the PAMINA benchmark calculations [Refs. 3 and 4] and results reported in the ANDRA Dossier 2005 Argile series [Refs.5, 6, and 7]. The present report includes the model description from the previous report [Ref. 2] and presents new calculations using the UFDC Clay GDSM "Baseline" Model for a selected set of hypothetical clay repository conditions and with waste packages each containing 32 PWR fuel assemblies having a variety of burnups.

---

[a] Spent nuclear fuel as defined in this report is nuclear fuel discharged from a reactor that has been deemed to have no economic value and is intended to be permanently disposed of in a geologic repository.

2.   MODEL DESCRIPTION

The development of a clay GDSM was initiated in FY09 under the FCT Separations/Waste Form campaign [Ref. 8]. The initial model, which focused on diffusive radionuclide transport through the far-field, served as the starting point for subsequent development which eventually culminated in the UFDC Clay GDSM described in Ref. 2 and in this section.

The development of the UFDC Clay GDSM centered on a requirement of being flexible to accommodate a variety of different scenarios. These scenarios range from different material properties, different waste forms with varying radionuclide inventories, and different repository and engineered barrier system designs. As such, tool development did not begin with defining a specific scenario around which models would be developed, but rather focused on developing modeling tools that could then be used to evaluate a wide range of alternative scenarios.

The UFDC Clay GDSM is envisioned primarily as a "stand-alone" tool, but includes the ability to link to external tools and ancillary calculations. The coupling of these models and their linkage to input data and the results of ancillary calculations and model output is shown in Figure 1. This report discusses the development of the UFDC Clay GDSM (orange box). Other analytic tools, models, and input information are being developed within the UFD Campaign or other campaigns within the Fuel Cycle Technologies (FCT) program (i.e., the Separations/Waste Form Campaign). As these tools are developed they can either be directly incorporated into future versions of the UFDC Clay GDSM or can link to it, as necessary.
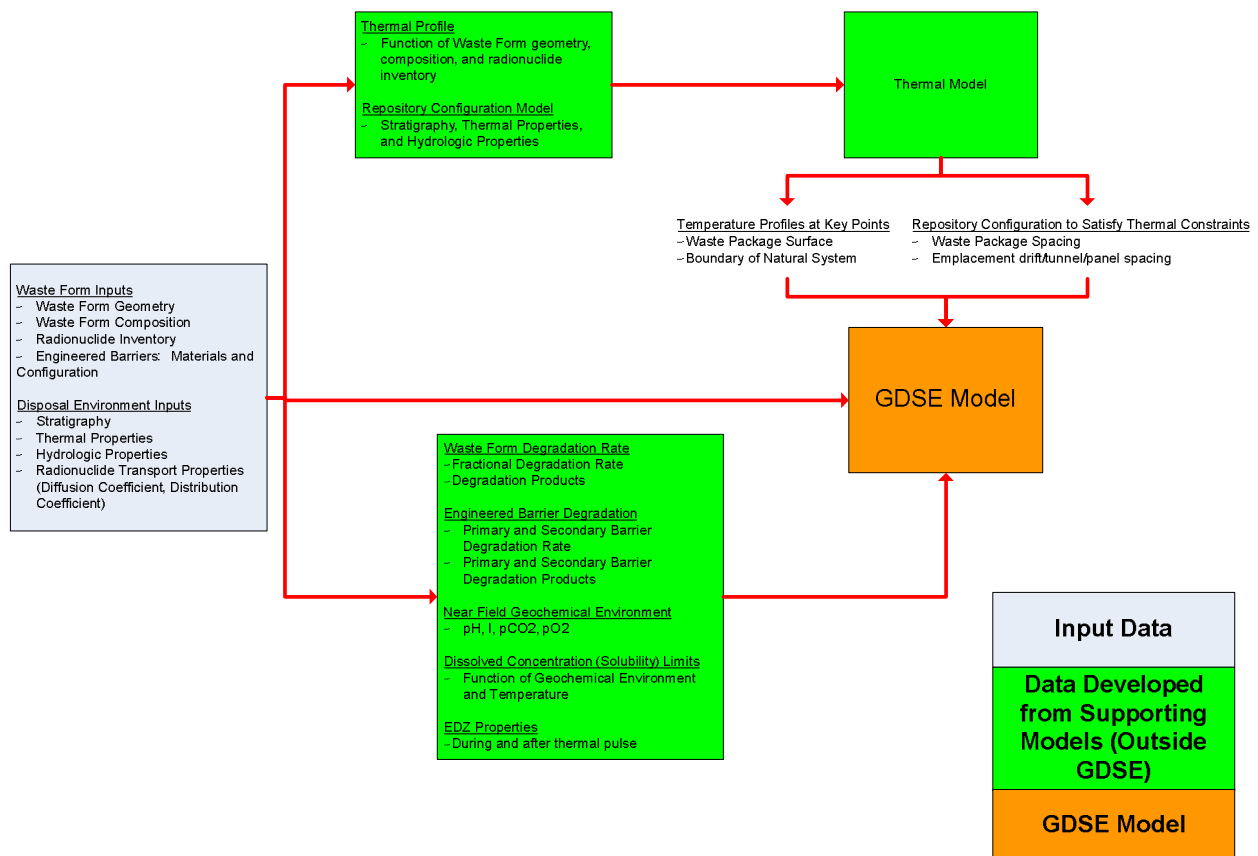
Figure 1. Clay GDSM Structure

The objective of the UFDC Clay GDSM is to integrate all of the key features, events, and processes (FEPs) for a clay generic disposal system into an integrated framework. It is developing using the GoldSim dynamic simulation software [Ref. 9], but is indented to be universally used by non-GoldSim practitioners through the use of the free GoldSim Player. All inputs are contained in a Microsoft Excel format that is linked to the GoldSim model. This allows the user the flexibility to evaluate multiple scenarios and conduct sensitivity analyses without having to make changes to the GoldSim model itself, rather only the input needs to be changed.

The overall linkage between the clay GDSM, the input spreadsheet, and the broad FEPs categories being used by the UFD campaign is shown in Figure 2.

The general components of the clay Long Term Repository Performance GDSM are:

- Source Term – waste form and radionuclide inventory
- Primary Engineered Barrier – waste package
- Secondary Engineered Barrier – buffer or other material surrounding a waste package
- Excavation Damage Zone (EDZ) – host rock effected by facility construction and the emplacement of waste
- Far Field – host rock not affected by the emplacement of waste
- Fast Pathways – generic capability to simulate the presence of fast pathways either intersecting the emplaced waste or occurring at some location within the far field (either directly intersecting the waste or the engineered barrier system, or effecting far-field transport behavior).
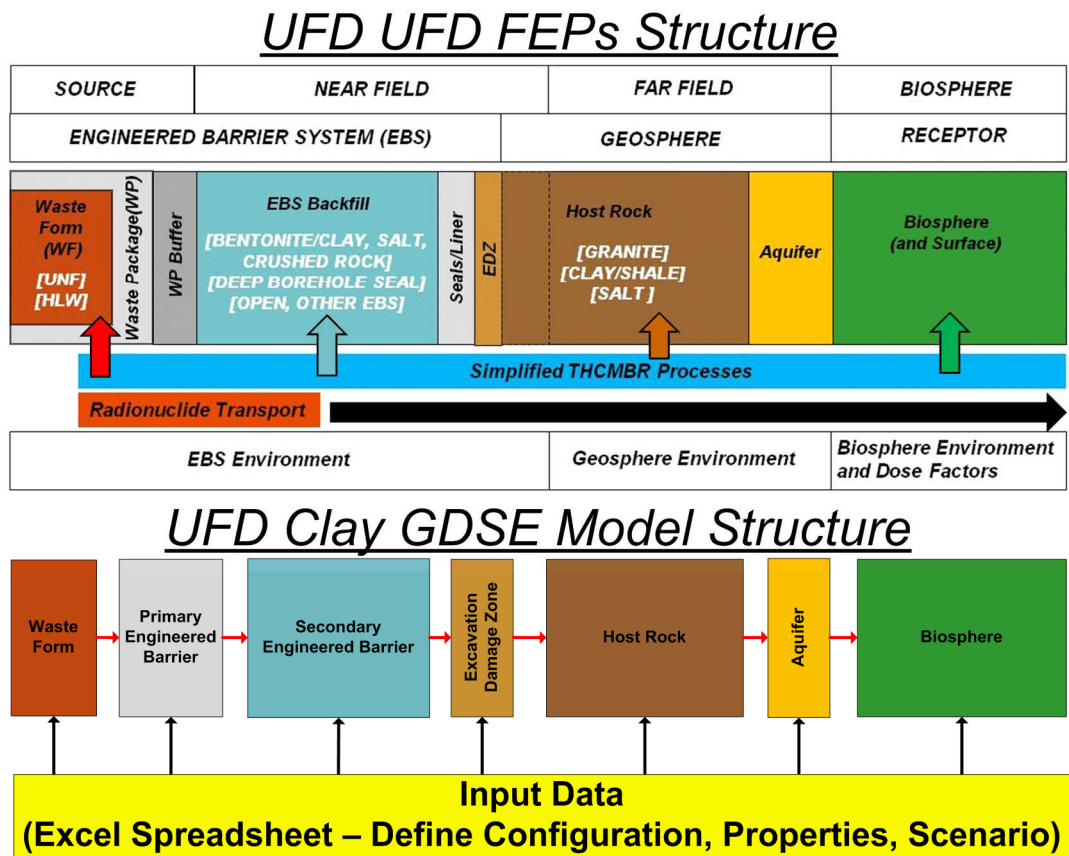
Figure 2. Clay Long-Term Repository Performance GDSM Linkages

2.1   Overall Model Framework

The underlying basis behind the UFDC Clay GDSM is a "waste unit cell." Except near the edges, repository designs in general are repeatable configurations of emplaced waste separated by constant distances on the horizontal plane. This symmetry allows for the development of simplified two-dimensional representations of an emplacement location and the surrounding natural media. A wide range of configurations can be modeled using the same overall modeling framework by changing input parameters. This is shown schematically in Figure 3 for different conceptualizations of waste emplacement.

The "waste unit cell" is defined by a width, height, and depth as shown in Figure 3. The Clay GDSM assumes one-dimensional radionuclide transport within the engineered barrier system and two-dimensional radionuclide transport (x – z plane in Figure 3) in the far-field. The domain height (z direction in Figure 3) represents the height to an overlying conductive flow unit (an aquifer) where a swept away boundary condition is applied. A zero flux boundary condition is applied at the bottom of the far-field domain and a symmetry boundary condition (zero flux) is applied at the sides of the far-field domain.

The depth (y plane in Figure 3) represents the distance between adjacent waste emplacements and is used to determine engineered barrier system component volumes and resultant radionuclide concentrations.

In evaluating a specific site and design, more elaborate models would likely be used to evaluate three-dimensional and non-symmetric effects. However, the use of symmetrical and prescribed boundary conditions is appropriate when using simplified modeling tools to evaluate generic sites.
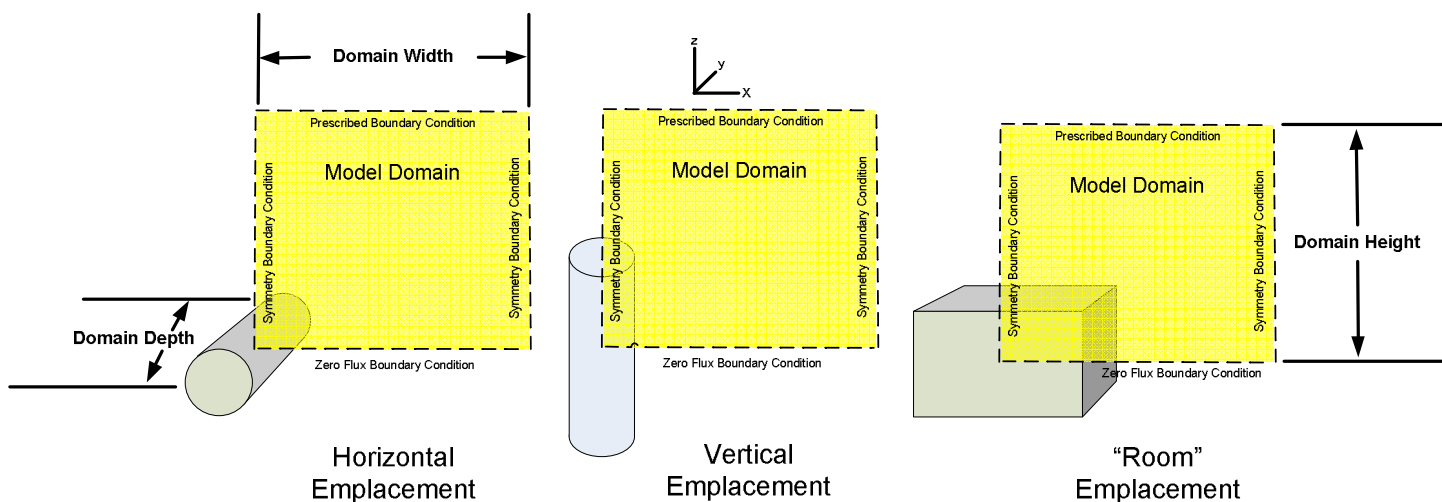
Figure 3. Conceptual Framework for Clay GDSM

2.2   Source Term, Degraded Waste Form, Primary and Secondary Engineered Barriers

The source term, degraded waste form, and degraded primary engineered barrier components of the UFDC Clay GDSM are shown schematically in Figure 4 and the secondary engineered barrier component is shown schematically in Figure 5. Also shown on are the data and ancillary calculation/modeling results that serve as input to the model. As discussed previously, the user has the capability to change the input parameters through the GDSM input spreadsheet and thus is able to model a wide variety of alternatives within the engineered system of a generic clay conceptual repository design.

2.2.1   Radionuclide Inventory

The source term for the UFDC Clay GDSM begins with the inventory. The model includes 36 radionuclides important to repository performance. These are input into the model from a spreadsheet as shown in Table 1 as constants that represent the inventory emplaced in a "single waste unit cell". A multiplier that can be used to conduct inventory-related sensitivity studies is also included on the input spreadsheet.

Table 1. Radionuclide Inventory.

Inventory Multiplier	1.00E+00		
Isotope	**Mass (g / Waste Unit Cell)**	**Isotope**	**Mass (g / Waste Unit Cell)**
Ac227	0.00E+00	Pu242	1.03E+01
Am241	1.81E+03	Ra226	0.00E+00
Am243	1.19E+03	Ra228	0.00E+00
C14	1.00E+00	Sb126	0.00E+00
Cl36	0.00E+00	Se79	0.00E+00
Cm245	4.21E+01	Sn126	2.20E+02
Cs135	3.39E+03	Sr90	3.54E+03
Cs137	8.19E+03	Tc99	5.63E+03
I129	0.00E+00	Th229	2.38E-05
Nb93	3.15E+03	Th230	2.24E-02
Np237	5.28E+03	Th232	6.91E-03
Pa231	0.00E+00	U232	7.06E-06
Pb210	0.00E+00	U233	3.78E-06
Pd107	0.00E+00	U234	1.76E-01
Pu238	1.58E+00	U235	4.73E+00
Pu239	2.46E+01	U236	5.49E+00
Pu240	6.04E+02	U238	8.02E-01
Pu241	3.32E+00	Zr93	0.00E+00

Note that the inventory values shown are for example only.

Properties of Degraded Primary
Engineered Barrier
- Dimensions
- Density
- Porosity
- Distribution Coefficients
- Solubility limits

Degraded Primary Engineered Barrier Radionuclide Transport Model Calculations
- Volume of cell – Static, No Uncertainty
- Dissolved Concentration Limits – Uncertain / Static / Isothermal
- Radionuclide Sorption – Uncertain / Static / Isothermal
- Advective Flow Properties: Volumetric Flow Rate - Static, No Uncertainty
- Diffusive Transport Properties: Diffusive Length and Area Static, No Uncertainty; Effective Diffusion Coefficient Solely a Function of Porosity (and Free Diffusion Coefficient in Water)

Inventory
- Data vector by species
- Mass Per "Unit Cell" (no uncertainty)
- No gap/grain boundary fraction
- Inventory Multiplier (for sensitivity analysis)

Degraded Primary Engineered Barrier Materials
- Degraded Primary EB Solid
- Degraded Primary EB Water

Waste Form Degradation
- Fractional Degradation \ Rate (no uncertainty)

SOURCE MODEL

DEGRADED WASTE FORM
Mixing Cell
(Diffusion and Advection)

DEGRADED PRIMARY ENGINEERED BARRIER
Mixing Cell
(Diffusion and Advection)

SECONDARY ENGINEERED BARRIER

Primary Engineered Barrier Degradation
- Single or Multiple Primary Barriers
- Primary Barrier Failure Time (all fail at the same time, no uncertainty)

Degraded Waste Form Materials
- Degraded Waste Form Solid
- Degraded Waste Form Water

Properties of Degraded Waste Form
- Dimensions
- Density
- Porosity
- Distribution Coefficients
- Solubility limits

Degraded Waste Form Radionuclide Transport Model Calculations
- Volume of cell – Static, No Uncertainty
- Dissolved Concentration Limits – Uncertain / Static / Isothermal
- Radionuclide Sorption – Uncertain / Static / Isothermal
- Advective Flow Properties: Volumetric Flow Rate - Static, No Uncertainty
- Diffusive Transport Properties: Diffusive Length and Area Static, No Uncertainty; Effective Diffusion Coefficient Solely a Function of Porosity (and Free Diffusion Coefficient in Water)

Figure 4. Schematic of Source Term, Degraded Waste Form, and Primary Engineered Barrier Representation.

Figure 5. Schematic of Secondary Engineered Barrier Representation.

2.2.2   Waste Form and Primary Engineered Barrier

The configuration of the engineered barriers is controlled from the input spreadsheet as shown in Table 2. A parameter is included to change the number of discrete units that are represented by the single "unit cell" within the UFDC Clay GDSM. This allows the user to simulate the disposal of waste at multiple identical locations within the model.

Table 2. Waste Form and Primary Engineered Barrier Parameters.

General	
Number of Discrete Units (i.e., waste packages) Represented	1
Waste Form	
Waste Form Fractional Degradation Rate (yr^{-1})	1.00E-05
Primary Engineered Barrier (i.e., Waste Package)	
Primary Engineered Barrier Present (0=no; 1=yes)	1
Waste Package Failure Time (years)	30,000

Note that the values shown are for example only.

A parameter (flag) is used to define if a primary engineered barrier is included. If it is assumed that no primary barrier is present waste form degradation is assumed to immediately begin when the simulation is initiated. If a primary engineered barrier is included, its failure is represented as a single failure mode where the barrier fails completely at a defined time, exposing the waste form. If the UFDC Clay GDSM is being used to represent multiple identical waste disposal locations, it is assumed that the primary engineered barrier at each of these locations fails at the same time.

The degradation of the waste form degradation is currently represented as a single fractional degradation rate that does not vary with time. The UFDC Clay GDSM assumes congruent release of all radionuclides as the waste degrades (i.e., gap/grain boundary radionuclide release from directly disposed fuel is not considered).

The UFDC Clay GDSM assumes one-dimensional radionuclide transport through the waste form and primary engineered barrier with each being modeled as single batch-reactor mixing cells. The properties of the waste form and primary engineered barrier are shown in Table 3 and are input as scalar values that do not change with time. In general, it is expected that the fully degraded state of these barriers would be modeled; however the user can change the properties to represent different conditions.

The volume of water in each batch-reactor mixing cell is equal to the product of the volume of the cell and the porosity and the mass of solid is equal to the product of the volume of the cell and the density (assumed to be the dry density).

It is assumed that diffusion is the primary radionuclide transport mechanism in a clay disposal environment, so the batch-reactor mixing cells are diffusively coupled. However, to investigate the effects of advective transport through the engineered barriers, the mixing cells are also advectively linked with the model user able to change the advective flow rate (scalar value that does not change with time).

Table 3. Waste Form and Primary Engineered Barrier Properties.

Property	Waste Form	Primary Engineered Barrier
Material Density (kg/m^3)	4830	5240
Porosity	0.175	0.4
Volume (m^3)	2.6	0.400
Thickness (m)	0.40	0.03
Diffusion Area (m^2)	12.7	13.8
Advective Flow Rate (m^3/yr)	0.00E+00	0.00E+00

Note that the values shown are for example only.

The diffusive area and diffusion length are input parameters as shown in Table 3. The effective diffusive coefficient is given as:

$$D_{eff,j} = D_{ref} \bullet R_{D,j} \bullet \phi$$

where

$D_{eff,j}$ = Effective diffusion coefficient for element j (m^2/yr)

D_{ref} = Reference diffusivity in water (m^2/yr)

$R_{D,j}$ = Relative diffusivity in water for element j

ϕ = Porosity

The reference diffusivity and the element-specific relative diffusivity in water, shown in Table 4, are user inputs (scalar values).

The ability to simulate dissolution/precipitation and reversible sorption is included in each batch-reactor mixing cell. It is assumed that the dissolved concentration limits and distribution coefficients are represented in the UFDC Clay GDSM as log-triangular, as shown in Table 5, with the user having the ability to define the minimum, best estimate, and maximum values of the distribution from the input spreadsheet for the waste form and primary engineered barrier (separate input tables for each barrier).

For scenarios where the degraded waste form, the degraded primary engineered barrier, or both are **NOT** considered, parameters in the input spreadsheet can be defined to force immediate transport through the mixing cells by:

- Setting the cell volumes to a very small number (i.e., 10^{-5} m^3);
- Setting the advective flow rate out of the mixing cell to a very large number (i.e., 10^{10} m^3/yr)
- Setting the dissolved concentration limit to a very large number (i.e., 10^{50} mol/L)
- Setting the distribution coefficients for each element to a very small number (i.e., 10^{-50} m^3/kg)

Table 4. Reference and Relative Diffusivity.

Radioelement	Relative Diffusivity	Radioelement	Relative Diffusivity
Ac	1.000	Pd	1.000
Am	0.413	Pu	0.565
C	0.513	Ra	0.387
Cl	0.883	Sb	1.000
Cm	1.000	Se	0.452
Cs	0.896	Sn	0.674
I	0.892	Sr	0.344
Nb	1.000	Tc	0.848
Np	0.269	Th	0.260
Pa	0.263	U	0.289
Pb	1.000	Zr	1.000
Reference Diffusivity ($m^2 s^{-1}$)		2.30E-09	

Note that the values shown are for example only.

Table 5. Dissolved Concentration Limit and Distribution Coefficient Parameters (Log-Triangular Distribution).

Element	Dissolved Concentration Limit (Mol/L)			Distribution Coefficient (m^3/Kg)		
	Minimum	Most Likely	Maximum	Minimum	Most Likely	Maximum
Actinium	4.00E-09	2.00E-06	2.00E-05	1.00E+00	5.00E+00	5.00E+00
Americium	3.00E-10	2.00E-09	1.00E-08	1.00E+00	5.00E+00	5.00E+00
Antimony	1.00E+50	1.00E+50	1.00E+50	1.00E-51	1.00E-50	1.00E-49
Carbon	9.70E-06	2.00E-04	2.00E-04	1.00E-02	1.00E-01	1.00E-01
Cesium	1.00E+50	1.00E+50	1.00E+50	1.00E-51	3.00E-01	3.00E-01
Chlorine	1.00E+50	1.00E+50	1.00E+50	1.00E-51	1.00E-50	1.00E-49
Curium	3.00E-10	2.00E-09	1.00E-08	1.00E-51	1.00E-50	1.00E-49
Iodine	1.00E+50	1.00E+50	1.00E+50	1.00E-51	1.00E-50	1.00E-49
Lead	3.00E-03	2.00E-02	2.00E-02	1.00E-51	1.00E-50	1.00E-49
Neptunium	3.00E-09	5.00E-09	1.00E-08	5.00E-01	1.00E+00	1.00E+00
Niobium	1.00E+50	1.00E+50	1.00E+50	1.00E-51	1.00E-50	1.00E-49
Paladium	8.00E-08	8.00E-07	8.00E-06	1.00E-51	1.00E-50	1.00E-49
Protactinium	1.00E-09	1.00E-08	1.00E-07	5.00E-01	1.00E+00	1.00E+00
Plutonium	1.00E-11	4.00E-11	2.00E-10	1.00E+00	5.00E+00	5.00E+00
Radium	1.00E-06	2.00E-02	2.00E-01	1.00E-51	5.00E-01	5.00E-01
Selenium	7.00E-06	1.00E-05	2.00E-05	1.00E-51	1.00E-50	1.00E-49
Strontium	1.00E-03	6.00E-03	6.01E-03	1.00E-51	2.00E-02	2.00E-02
Technetium	3.20E-07	1.00E-04	1.00E-04	1.00E-51	1.00E-50	1.00E-49
Thorium	8.00E-10	3.00E-09	1.00E-08	1.00E+00	5.00E+00	5.00E+00
Tin	1.00E-07	2.00E-07	2.00E-07	1.00E-51	1.00E-50	1.00E-49
Uranium	1.00E-08	5.00E-07	5.01E-07	1.00E-01	1.00E+00	1.00E+00
Zirconium	6.00E-07	6.00E-05	6.01E-05	1.00E-51	1.00E-50	1.00E-49

Note that the values shown are for example only.

2.2.3   Secondary Engineered Barrier

The UFDC Clay GDSM assumes one-dimensional radionuclide transport through the secondary engineered barrier using the linked batch-reactor mixing cell structure shown in Figure 5. This structure allows the user to select either a single- or a dual-continuum representation of radionuclide transport. This allows for the representation of a variety of secondary engineered barrier materials (i.e., bentonite or cementitious) with different radionuclide transport properties.

If a single-continuum representation is chosen, radionuclide transport through the secondary engineered barrier is represented by three linked batch-reactor mixing cells (top cell network shown in Figure 5) that span the thickness of the barrier. It is assumed that diffusion is the primary radionuclide transport mechanism in a clay disposal environment, so the batch-reactor mixing cells are diffusively coupled. However, to investigate the effects of advective transport through the engineered barriers, the mixing cells are also advectively linked with the model user able to input an advective flow rate.

If a dual-continuum representation is chosen, radionuclide transport through the secondary engineered barrier is represented by six linked batch-reactor mixing cells (shown in Figure 5). Three of the linked batch-reactor mixing cells (top cell network shown in Figure 5), that span the thickness of the barrier, represent the matrix continuum and three of the batch-reactor mixing cells (bottom cell network shown in Figure 5) represent the fracture continuum. It is assumed that diffusion is the primary radionuclide transport mechanism in a clay disposal environment, so the batch-reactor mixing cells representing the fracture continuum are diffusively coupled. The diffusion of radionuclides between the matrix and fracture continua is also included in the dual-continuum representation. To investigate the effects of advective transport through the engineered barriers, the dual- continuum representation advectively links the fracture cell network with the user able to input an advective flow rate. No advective flow through the matrix continua occurs in the dual-continuum representation.

The properties of the secondary engineered barrier are shown in Table 6. The volume, thickness, and perimeter of the secondary engineered barrier are input as scalar values and the porosity, density, tortuosity, fracture spacing, and fracture aperture are represented by log-triangular probability distributions. The properties also do not change with time. In general, it is expected that the fully degraded state of the secondary engineered barrier would be modeled; however the user can change the properties to represent different conditions.

The ability to simulate dissolution/precipitation and reversible sorption is included in each secondary engineered barrier batch-reactor mixing cell. It is assumed that the dissolved concentration limits and distribution coefficients are represented in the UFDC Clay GDSM as log-triangular, as shown in Table 5, with the user having the ability to define the minimum, best estimate, and maximum values of the distribution from the input spreadsheet for the secondary engineered barrier.

Single Continuum Representation

In the single continuum representation the volume of water in each batch-reactor mixing cell is equal to the product of the $1/3^{rd}$ the volume of the secondary engineered barrier and the porosity (3 mixing cells . The mass of solid material in the mixing cell is equal to the product of $1/3^{rd}$ the volume of the secondary engineered barrier and the density (assumed to be the dry density).

For the single-continuum representation, one-dimensional diffusive radionuclide transport is modeled assuming the diffusive area is equal to the product of the outer perimeter of the secondary engineered barrier and the model domain depth (see Figure 3). This diffusive area is applied to all three batch reactor mixing cells, resulting in a larger diffusive area than would result from a more explicit representation of the geometry. However, this approach will result in larger diffusive fluxes and is a conservative approximation. The diffusive length in each batch-reactor mixing cell is equal to $1/3^{rd}$ the thickness of the secondary engineered barrier.

The effective diffusion coefficient is given as:

$$D_{eff,j} = D_{ref} \bullet R_{D,j} \bullet \phi \bullet \tau \bullet \phi_{A,j}$$

where

$D_{eff,j}$	=	Effective diffusion coefficient for element j (m^2/yr)
D_{ref}	=	Reference diffusivity in water (m^2/yr); Table 4
$R_{D,j}$	=	Relative diffusivity in water for element j; Table 4
ϕ	=	Porosity
τ	=	Tortuosity
$\phi_{A,j}$	=	Available porosity for element j (0 to 1); Table 7

Table 6. Secondary Engineered Barrier Properties.

a) Scalar parameters

Property	Secondary Engineered Barrier
Volume (m^3)	18.0
Thickness (m)	0.6
Perimeter (m)	40
Advective Flow Rate (m^3/yr)	0.00E+00

b) Stochastic parameters

Property	Minimum	Most Likely	Maximum
Porosity	0.05	0.1	.15
Density (kg/m^3)	1971	2190	2409
Tortuosity	0.75	0.9	1
Fracture Spacing (m)	0.225	2.50E-01	0.275
Fracture Aperture (m)	0.004	0.005	0.006

Note that the values shown are for example only.

Fracture Spacing and Fracture Aperture are required only for a dual-continuum representation.

This approach for determining the effective diffusion coefficient provides flexibility to the user in representing diffusive radionuclide transport in the single-continuum representation of the secondary engineered barrier. As discussed above, both the reference diffusivity and the element-specific relative diffusivities in water are user inputs (Table 4). The element-specific available porosities are represented as triangular distributions with the minimum, most likely, and maximum values being user inputs, as shown in Table 7.

Table 7. Available Porosity.

Element	Minimum	Most Likely	Maximum	Element	Minimum	Most Likely	Maximum
Ac	0.998	0.999	1	Pd	0.998	0.999	1
Am	0.998	0.999	1	Pu	0.998	0.999	1
C	0.998	0.999	1	Ra	0.998	0.999	1
Cl	0.998	0.999	1	Sb	0.998	0.999	1
Cm	0.998	0.999	1	Se	0.998	0.999	1
Cs	0.998	0.999	1	Sn	0.998	0.999	1
I	0.998	0.999	1	Sr	0.998	0.999	1
Nb	0.998	0.999	1	Tc	0.998	0.999	1
Np	0.998	0.999	1	Th	0.998	0.999	1
Pa	0.998	0.999	1	U	0.998	0.999	1
Pb	0.998	0.999	1	Zr	0.998	0.999	1

Note that the values shown are for example only.

Dual Continuum Representation

The volume of water in the batch-reactor mixing cells that represent the matrix continuum, the mass of solid material in the mixing cell, the diffusive area, the diffusive length, and the effective diffusion coefficient are determined identical to the single-continuum representation discussed immediately above.

The conceptual representation of the fracture-continuum assumes equally spaced, through-going, parallel fractures along the outer perimeter of the secondary engineered barrier, as shown schematically in Figure 6.

The volume of water in the batch-reactor mixing cells that represent the fracture continuum is determined as:

$$V_W = \frac{P_{SECEB}}{F_s} \bullet F_A \bullet \frac{T_{SECEB}}{3} \bullet D_{domain} \qquad \text{Eq. 1}$$

where

V_W =   Volume of water in a fracture continuum batch-reactor mixing cell (m^3)

$P_{SEC\ EB}$ =   Outer perimeter of the secondary engineered barrier (m)

$T_{SEC\ EB}$ =   Thickness of the secondary engineered barrier (m); factor of three applied since there are three batch-reactor mixing cells spanning the thickness

F_S =   Fracture spacing along the outer perimeter of the secondary engineered barrier (m)

F_A =   Fracture aperture (m)

D_{Domain} =   Model domain depth (m); Figure 3
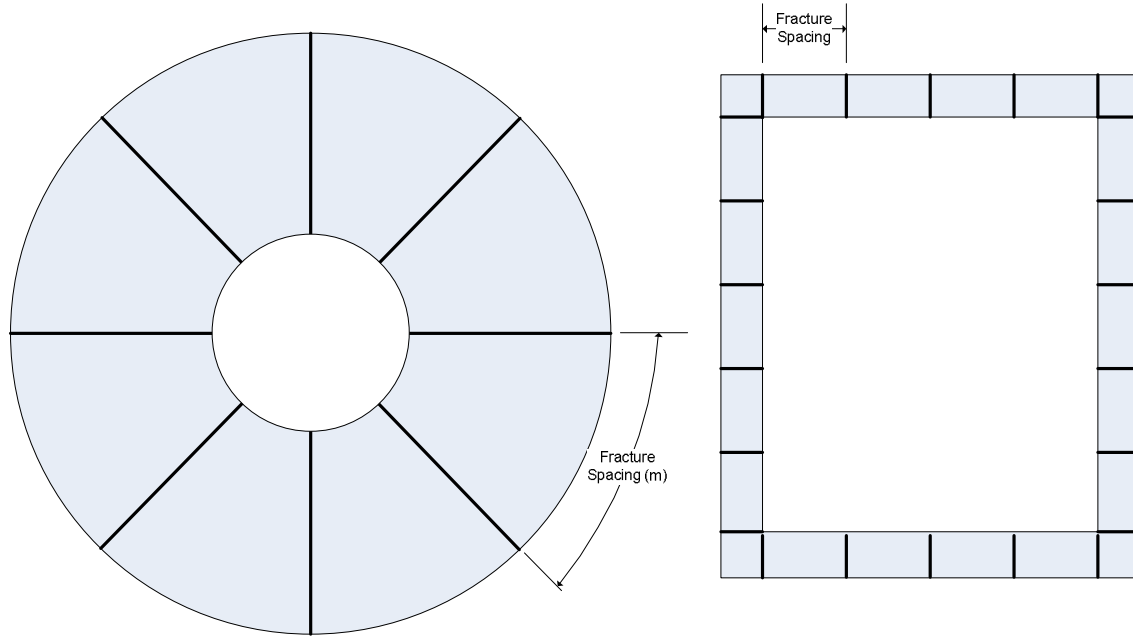
Figure 6. Schematic of Fracture Network Representation in the Secondary Engineered Barrier.

The diffusive length within each fracture-continua cell is equal to 1/3rd the thickness of the secondary engineered barrier and the diffusive area is determined as:

$$D_{A-F} = \frac{P_{SECEB}}{F_s} \bullet F_A \bullet D_{domain}$$ Eq. 2

where

D_{A-F}	=	Diffusive area in a fracture continuum batch-reactor mixing cell (m^2)
$P_{SEC\,EB}$	=	Outer perimeter of the secondary engineered barrier (m)
F_S	=	Fracture spacing along the outer perimeter of the secondary engineered barrier (m)
F_A	=	Fracture aperture (m)
D_{Domain}	=	Model domain depth (m); Figure 3

The diffusive area between the fracture and matrix continuums (matrix diffusion) is determined as:

$$D_{A-M} = \frac{P_{SECEB}}{F_s} \bullet 2 \bullet \frac{T_{SECEB}}{3} \bullet D_{domain}$$ Eq. 3

where

D_{A-M}	=	Diffusive area for matrix diffusion between the fracture and matrix continuum batch-reactor mixing cells (m^2)

$P_{SEC\,EB}$ = Outer perimeter of the secondary engineered barrier (m)

$T_{SEC\,EB}$ = Thickness of the secondary engineered barrier (m); factor of three applied since there are three batch-reactor mixing cells spanning the thickness, 2 surfaces for each fracture

F_S = Fracture spacing along the outer perimeter of the secondary engineered barrier (m)

D_{Domain} = Model domain depth (m); Figure 3

The diffusive length in the fracture continua batch-reactor mixing cell is assumed to be zero meters. The diffusive length in the matrix continua batch-reactor mixing cell is assumed to equal half the fracture spacing.

The effective diffusive coefficient in the water with the fracture continua batch-reactor mixing cells is given as:

$$D_{eff,j} = D_{ref} \bullet R_{D,j}$$
Eq. 4

where

$D_{eff,j}$ = Effective diffusion coefficient for element j (m^2/yr)

D_{ref} = Reference diffusivity in water (m^2/yr); Table 4

$R_{D,j}$ = Relative diffusivity in water for element j; Table 4

For scenarios where the secondary engineered barrier is not considered, parameters in the input spreadsheet can be defined to force immediate transport through the mixing cells by:

- Selecting single-continuum for representing radionuclide transport
- Setting the cell volumes to a very small number (i.e., 10^{-5} m^3);
- Setting the advective flow rate out of the mixing cell to a very large number (i.e., 10^{10} m^3/yr)
- Setting the dissolved concentration limit to a very large number (i.e., 10^{50} mol/L)
- Setting the distribution coefficients for each element to a very small number (i.e., 10^{-50} m^3/kg)

2.3 Near Field/Excavation Damage Zone

The near field/EDZ component of the UFDC Clay GDSM is shown schematically in Figure 7. Also shown are the data and ancillary calculation/modeling results that serve as input to the model. As discussed previously, the user has the capability to change the input parameters through the GDSM input spreadsheet and thus is able to model a wide variety of near field/EDZ conditions within generic clay media. The linkage between the secondary engineered barrier and the EDZ is shown in Figure 8.

The UFDC Clay GDSM assumes one-dimensional radionuclide transport through the EDZ using the linked batch-reactor mixing cell structure shown in Figure 7. This structure allows the user to select either a single- or a dual-continuum representation of radionuclide transport. This allows for the representation of a variety of EDZ conditions with different radionuclide transport properties.

If a single-continuum representation is chosen, radionuclide transport through the EDZ is represented by three linked batch-reactor mixing cells (top cell network shown in Figure 7) that span the EDZ thickness.
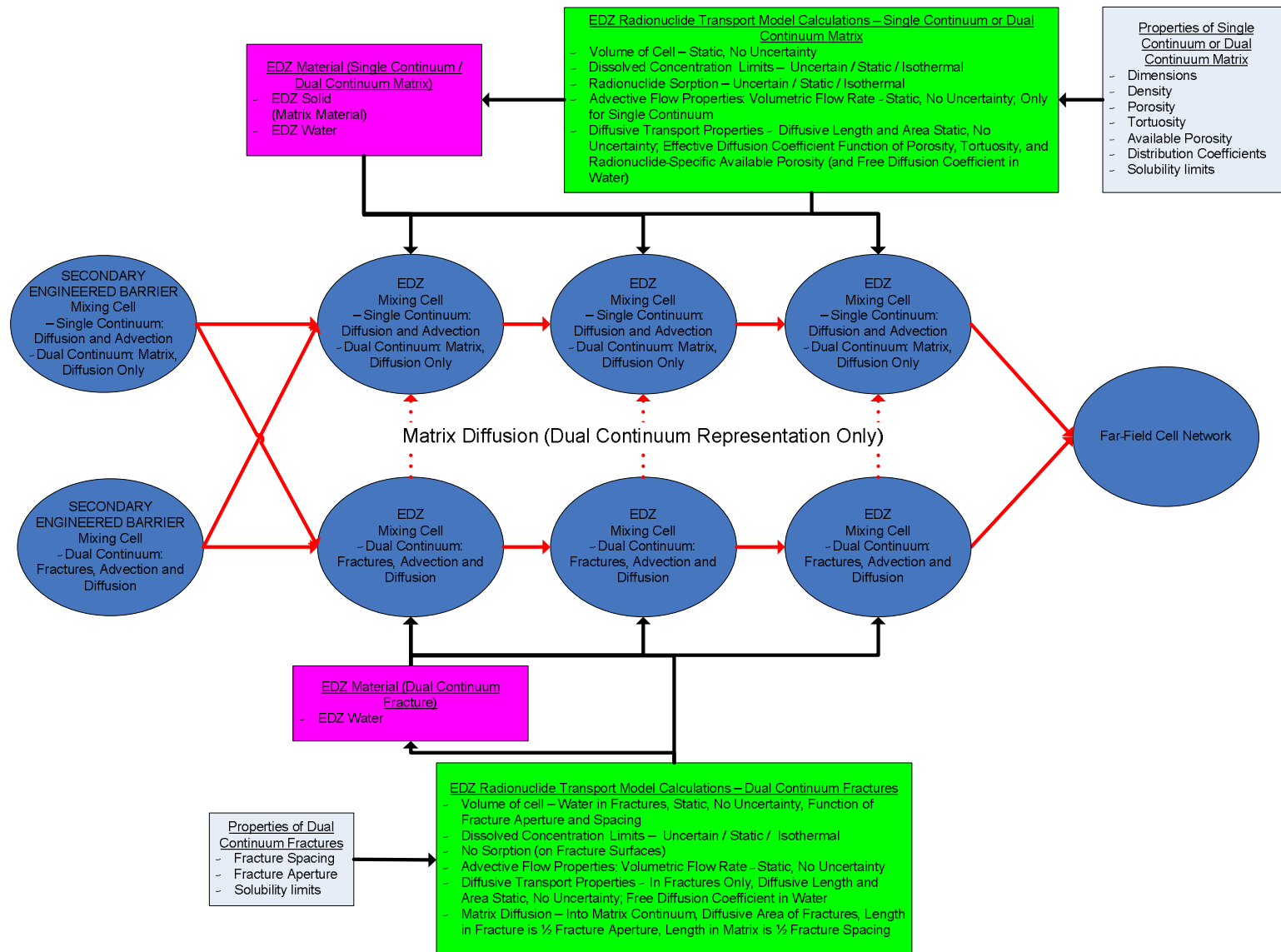
Figure 7. Schematic of Near Field/Excavation Damage Zone Representation.

It is assumed that diffusion is the primary radionuclide transport mechanism in a clay disposal environment, so the batch-reactor mixing cells are diffusively coupled. However, to investigate the effects of advective transport through the engineered barriers, the mixing cells are also advectively linked with the model user able to input an advective flow rate. If a dual-continuum representation is chosen, radionuclide transport through the EDZ is represented by six linked batch-reactor mixing cells (shown in Figure 7). Three of the linked batch-reactor mixing cells (top cell network shown in Figure 7), that span the thickness of the EDZ, represent the matrix continuum and three of the batch-reactor mixing cells (bottom cell network shown in Figure 7) represent the fracture continuum. It is assumed that diffusion is the primary radionuclide transport mechanism in a clay disposal environment, so the batch-reactor mixing cells representing the fracture continuum are diffusively coupled. The diffusion of radionuclides between the matrix and fracture continua is also included in the dual-continuum representation. To investigate the effects of advective transport through the engineered barriers, the dual- continuum representation advectively links the fracture cell network with the user able to input an advective flow rate. No advective flow through the matrix continua occurs in the dual-continuum representation.

The properties of the EDZ are shown in Table 8. The volume, thickness, and perimeter of the EDZ are input as scalar values and the porosity, density, tortuosity, fracture spacing, and fracture aperture are represented by log-triangular probability distributions. The properties also do not change with time. In general, it is expected that the fully degraded state of the EDZ would be modeled; however the user can change the properties to represent different conditions.

The ability to simulate dissolution/precipitation and reversible sorption is included in each EDZ barrier batch-reactor mixing cell. It is assumed that the dissolved concentration limits and distribution coefficients are represented in the UFDC Clay GDSM as log-triangular, as shown in Table 4, with the user having the ability to define the minimum, best estimate, and maximum values of the distribution from the input spreadsheet for the secondary engineered barrier.

Table 8. Excavation Damage Zone Properties.

a) Scalar parameters

Property	Excavation Damage Zone
Volume (m^3)	270
Thickness (m)	1.15
Perimeter (m)	6.9
Advective Flow Rate (m^3/yr)	2.8E-06

b) Stochastic parameters

Property	Minimum	Most Likely	Maximum
Porosity	0.15	0.18	0.20
Density(kg/m^3)	2000	2250	2500
Tortuosity	0.5	0.75	1.0
Fracture Spacing (m)	0.25	0.5	1
Fracture Aperture (m)	0.0005	0.001	0.005

Note that the values shown are for example only.

Fracture Spacing and Fracture Aperture are required only for a dual-continuum representation.

Single Continuum Representation

In the single continuum representation the volume of water in each batch-reactor mixing cell is equal to the product of the 1/3rd the volume of the EDZ and the porosity (3 mixing cells . The mass of solid material in the mixing cell is equal to the product of 1/3rd the volume of the EDZ and the density (assumed to be the dry density).

For the single-continuum representation, one-dimensional diffusive radionuclide transport is modeled assuming the diffusive area is equal to the product of the outer perimeter of the EDZ and the model domain depth (see Figure 3). This diffusive area is applied to all three batch reactor mixing cells, resulting in a larger diffusive area than would result from a more explicit representation of the geometry. However, this approach will result in larger diffusive fluxes and is a conservative approximation. The diffusive length in each batch-reactor mixing cell is equal to 1/3rd the thickness of the EDZ.

The effective diffusion coefficient is given as:

$$D_{eff,j} = D_{ref} \bullet R_{D,j} \bullet \phi \bullet \tau \bullet \phi_{A,j}$$ Eq. 5

where

$D_{eff,j}$	=	Effective diffusion coefficient for element j (m^2/yr)
D_{ref}	=	Reference diffusivity in water (m^2/yr); Table 4
$R_{D,j}$	=	Relative diffusivity in water for element j; Table 4
ϕ	=	Porosity
τ	=	Tortuosity
$\phi_{A,j}$	=	Available porosity for element j (0 to 1); Table 7

This approach for determining the effective diffusion coefficient provides flexibility to the user in representing diffusive radionuclide transport in the single-continuum representation of the EDZ. As discussed above, both the reference diffusivity and the element-specific relative diffusivities are user inputs. The element-specific available porosities are represented as triangular distributions with the minimum, most likely, and maximum values being user inputs, as shown in Table 7 (identical input table for the EDZ).

Dual Continuum Representation

The volume of water in the batch-reactor mixing cells that represent the matrix continuum, the mass of solid material in the mixing cell, the diffusive area, the diffusive length, and the effective diffusion coefficient are determined identical to the single-continuum representation discussed immediately above.

The conceptual representation of the fracture-continuum assumes equally spaced, through-going, parallel fractures along the outer perimeter of the EDZ, as shown schematically in Figure 6.

The volume of water in the batch-reactor mixing cells that represent the fracture continuum is determined as:

$$V_W = \frac{P_{EDZ}}{F_s} \bullet F_A \bullet \frac{T_{EDZ}}{3} \bullet D_{domain}$$ Eq. 6

where

V_W	=	Volume of water in a fracture continuum batch-reactor mixing cell (m^3)
P_{EDZ}	=	Outer perimeter of the EDZ (m)
T_{EDZ}	=	Thickness of the EDZ (m); factor of three applied since there are three batch-reactor mixing cells spanning the thickness
F_S	=	Fracture spacing along the outer perimeter of the EDZ (m)
F_A	=	Fracture aperture (m)
D_{Domain}	=	Model domain depth (m); Figure 3

The diffusive length within each fracture-continua cell across the thickness of the EDZ is equal to 1/3rd the thickness. The diffusive area perpendicular to the fracture network is determined as:

$$D_{A-F} = \frac{P_{EDZ}}{F_s} \bullet F_A \bullet D_{domain} \qquad \text{Eq. 7}$$

where

$D_{A\text{-}F}$	=	Diffusive area in a fracture continuum batch-reactor mixing cell (m^2)
P_{EDZ}	=	Outer perimeter of the secondary engineered barrier (m)
F_S	=	Fracture spacing along the outer perimeter of the secondary engineered barrier (m)
F_A	=	Fracture aperture (m)
D_{Domain}	=	Model domain depth (m); Figure 3

The representation of matrix diffusion between the fracture and matrix continuums (matrix diffusion) determines the diffusive area as:

$$D_{A-M} = \frac{P_{EDZ}}{F_s} \bullet 2 \bullet \frac{T_{EDZ}}{3} \bullet D_{domain} \qquad \text{Eq. 8}$$

where

$D_{A\text{-}M}$	=	Diffusive area for matrix diffusion between the fracture and matrix continuum batch-reactor mixing cells (m^2)
P_{EDZ}	=	Outer perimeter of the secondary engineered barrier (m)
T_{EDZ}	=	Thickness of the secondary engineered barrier (m); factor of three applied since there are three batch-reactor mixing cells spanning the thickness, 2 surfaces for each fracture
F_S	=	Fracture spacing along the outer perimeter of the secondary engineered barrier (m)
D_{Domain}	=	Model domain depth (m); Figure 3

The diffusive length in the fracture continua batch-reactor mixing cell is assumed to be zero meters. The diffusive length in the matrix continua batch-reactor mixing cell is assumed to equal half the fracture spacing.

The effective diffusive coefficient in the water with the fracture continua batch-reactor mixing cells is given as:

$$D_{eff,j} = D_{ref} \bullet R_{D,j}$$
Eq. 9

where

$D_{eff,j}$ =   Effective diffusion coefficient for element j (m^2/yr)

D_{ref} =   Reference diffusivity in water (m^2/yr); Table 4

$R_{D,j}$ =   Relative diffusivity in water for element j; Table 4

This effective diffusion coefficient is used to both represent one-dimensional diffusion along the fracture network and matrix diffusion with the water-containing fracture, perpendicular to the fracture network. The effective diffusion coefficient for representing matrix diffusion perpendicular to the fracture network within the matrix continuum is determined identical to the single-continuum representation discussed immediately above

For scenarios where the EDZ is not considered, parameters in the input spreadsheet can be defined to force immediate transport through the mixing cells by:

- Selecting single-continuum for representing radionuclide transport

- Setting the cell volumes to a very small number (i.e., 10^{-5} m^3);

- Setting the advective flow rate out of the mixing cell to a very large number (i.e., 1,010 m^3/yr)

- Setting the dissolved concentration limit to a very large number (i.e., 1,050 mol/L)

- Setting the distribution coefficients for each element to a very small number (i.e., 10 to 50 m^3/kg)

2.4 Far Field

The far field component of the UFDC Clay GDSM is shown schematically in Figure 9. This formulation consists of 20x20 node network of batch-reactor mixing cells used to represent two-dimensional radionuclide transport. Releases from the near field enter the far field at the corner of the far field cell network. Radionuclide transport is assumed to occur primarily via diffusive mechanisms. However, the model includes advective coupling between the mixing cells to evaluate sensitivity.

The following assumptions are inherent in this model.

- The "depth" of each mixing cell equals the "depth" of the unit cell within the model (i.e., distance between the centers of single waste packages in a horizontal emplacement conceptual design)

- Reflective boundary conditions at 1) the center of each emplacement drift/tunnel, 2) at the centerline between emplacement drifts/tunnels, and 3) at the plane of the emplacement drifts.

- Dissolved concentration limits are applied in each mixing cell.

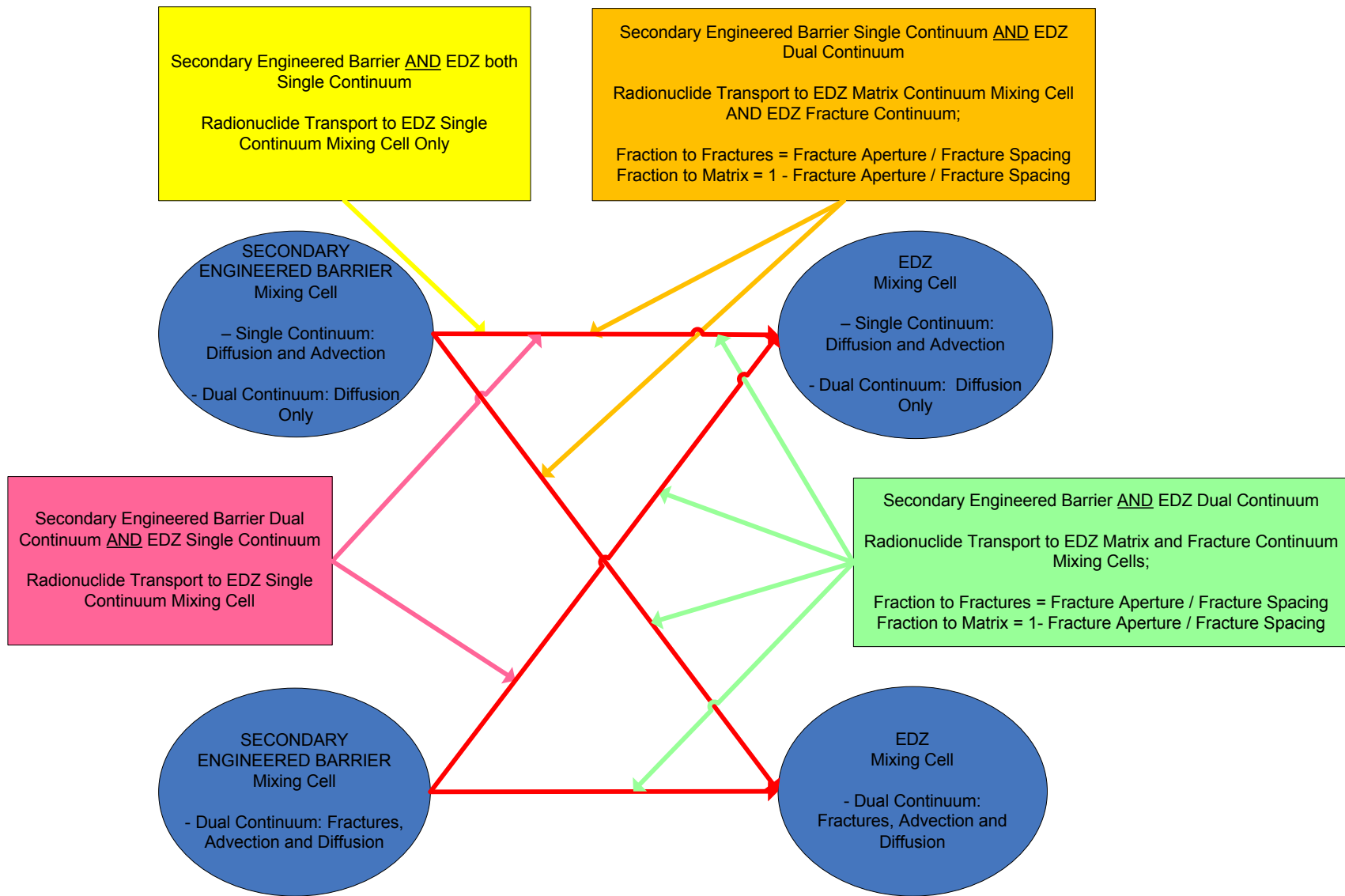- Reversible sorption in each mixing cell.

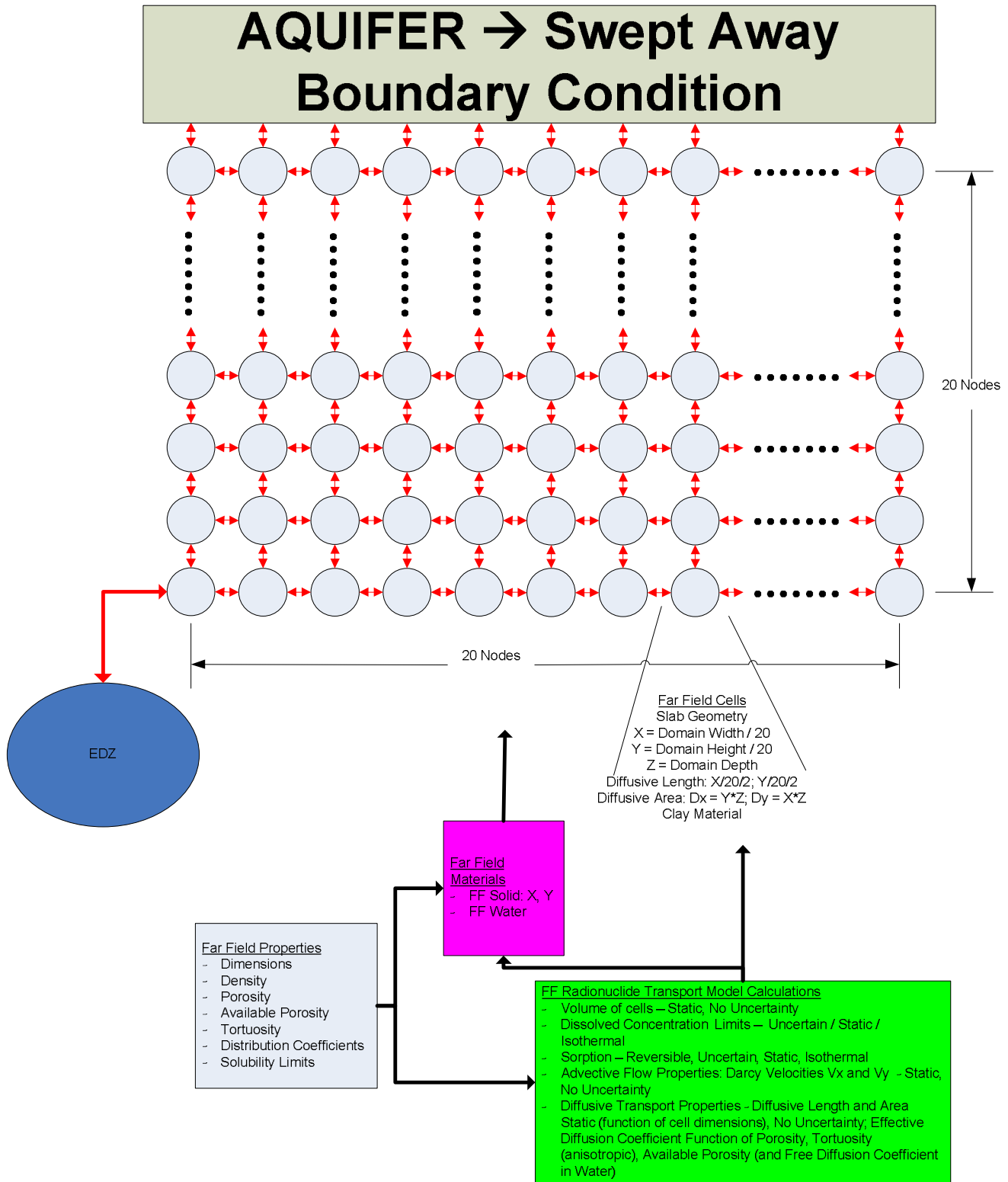Figure 8. Linkage Between the Secondary Engineered Barrier and the EDZ.

Figure 9. Schematic of Far Field Representation.

As discussed above (Figure 3), the far field domain height, width, and depth are represented parametrically within the model and are defined by the user. Thus, the model is extremely flexible and can accommodate different repository configurations (e.g., spacing of emplaced waste). Thermal modeling and analysis tools could be used to determine allowable configurations for a prescribed waste form and conceptual repository design that would then be input into the UFDC Clay GDSM.

The properties included in the far field component of the UFDC Clay GDSM are shown in Table 9. The porosity, density, and tortuosity of the far-field media are represented as triangular distributions with the minimum, most likely, and maximum values being input parameters. Different values for tortuosity can be defined in the horizontal and vertical directions to represent anisotropic diffusive radionuclide transport.

Table 9. Far Field Properties.

Property	Minimum	Most Likely	Maximum
Porosity	0.15	0.20	0.25
Density (kg/m^3)	2000	2250	2500
Tortuosity : X-dimension	0.5	0.75	0.1
Tortuosity : Y-dimension	0.25	0.5	0.75

Note that the values shown are for example only.

The volume of each batch-reactor mixing cell is determined assuming each cell is a rectangular parallelepiped as:

$$V_{cell} = \frac{W_{domain}}{20} \bullet \frac{H_{domain}}{20} \bullet D_{domain}$$

Eq. 10

where

V_{cell} =   Volume of each cell in the 20×20 node grid (m^3)

W_{domain} =   Width of the model domain (m); see Figure 3

H_{domain} =   Height of the model domain (m); see Figure 3

D_{domain} =   Depth of the model domain (m); see Figure 3

The volume of water in each batch-reactor mixing cell is equal to the product of the cell volume and the porosity. The mass of solid material in the mixing cell is equal to the product of the volume of the cell and the density (assumed to be the dry density).

The ability to simulate dissolution/precipitation and reversible sorption is also included in each far field batch reactor mixing cell in the same manner as was discussed above for the engineered barrier system and EDZ cells. Again, the model can be modified in the future should future investigations indicate that different probability distributions should be used or to involve explicit coupling to geochemical conditions and temperature within the batch reactor mixing cells.

Two-dimensional diffusion is modeled with the diffusive area and diffusive length in the horizontal and vertical directions determined as:

Diffusive Direction	Diffusive Area	Diffusive Length
Horizontal	$\dfrac{H_{domain}}{20} \bullet D_{domain}$	$\dfrac{W_{domain}}{20}$
Vertical	$\dfrac{W_{domain}}{20} \bullet D_{domain}$	$\dfrac{H_{domain}}{20}$

The effective diffusion coefficient is given as:

$$D_{eff,j} = D_{ref} \bullet R_{D,j} \bullet \phi \bullet \tau \bullet \phi_{A,j} \qquad \text{Eq. 11}$$

where

$D_{eff,j}$	=	Effective diffusion coefficient for element j (m^2/yr)
D_{ref}	=	Reference diffusivity in water (m^2/yr); Table 4
$R_{D,j}$	=	Relative diffusivity in water for element j; Table 4
ϕ	=	Porosity
τ	=	Tortuosity
$\phi_{A,j}$	=	Available porosity for element j (0 to 1); Table 7

This approach for determining the effective diffusion coefficient provides flexibility to the user in representing diffusive radionuclide transport in the far-field. As discussed above, both the reference diffusivity and the element-specific relative diffusivities are user inputs. The element-specific available porosities are represented as triangular distributions with the minimum, most likely, and maximum values being user inputs as shown in Table 7. To represent anisotropic diffusive radionuclide transport, different values for the available porosity can be defined in the horizontal and vertical directions.

As discussed above, the far-field component of the UFDC Clay GDSM includes advective links between the batch-reactor cells in both the horizontal and vertical directions. Darcy velocities (V_x, V_z; m/yr) can be entered in both the vertical and horizontal directions. The volumetric flow rates are determined as:

Advective Direction	Volumetric Flow Rate (m^3/yr)
Horizontal	$V_x \bullet \dfrac{H_{domain}}{20} \bullet D_{domain}$
Vertical	$V_z \bullet \dfrac{W_{domain}}{20} \bullet D_{domain}$

2.5 Aquifer

The Aquifer in the UFDC Clay GDSM is represented as a swept away boundary condition to the far-field cell network. The radionuclide mass flux reaching the aquifer is used to determine the annual dose to the receptor. The mass flux for each radionuclide (g/yr) is multiplied by the specific activity (Bq/g) to determine the activity flux (Bq/yr) entering the aquifer.

2.6 Biosphere

Radiation exposure, or dose, is used as a performance metric in the UFDC Clay GDSM. Biosphere dose conversion factors developed in the International Atomic Energy Agency's (IAEA) BIOMASS project for a simple drinking water well pathway (ERB 1) were used Ref. 10. This biosphere is described as:

> Example Reference Biosphere 1 (ERB 1) is deliberately designed to be very simple, being focused on a simple biosphere system and single exposure pathway. It is characterized by a drinking water well bored through the overburden into an aquifer that has been contaminated by radionuclide releases from the repository. Previous experience from more comprehensive biosphere modelling studies has shown that a drinking water well may sometimes represent a significant or even, depending on other aspects of the assessment context, a dominant pathway for release and exposure.

The results presented in this report should not be construed as being indicative of the true performance of a disposal system or compared to any regulatory performance objectives regarding repository performance for the following reasons:

- The UFDC Clay GDSM is very simplistic and do not include many of the features, events, and processes that need to be considered in an assessment of disposal system performance.

- The determination of biosphere dose conversion factors does not depend on the generic disposal environment, but rather on the biosphere beyond the generic disposal environment, the habits of the population in that biosphere, and potentially the regulatory framework. A variety of biospheres and local populations could be present over a given clay generic disposal environment and the resulting dose conversion factors may vary significantly.

Nevertheless, in lieu of a specific site, the reference biosphere allows for the assessment of generic disposal systems environments using a common, representative biosphere.

The parameters for the ERB 1 biosphere are provided in Table 10. The biosphere dose conversion factor is given as:

$$BDCF_j = DCF_j \bullet \frac{CR}{DF}$$ Eq. 12

where

$BDCF_j$ =   Biosphere dose conversion factor for element j (Sv/yr / Bq/yr)

DCF_j =   Dose conversion factor for element j (Sv/Bq); Table 10

CR =   Consumption rate assumed in the IAEA ERB 1 biosphere (m^3/yr); Table 10

DF =   Dilution factor assumed in the IAEA ERB 1 biosphere (m^3/yr); Table 10

Table 10. Biosphere Dose Conversion Parameters – IAEA Example Reference Biosphere 1.

Dilution Factor (m³/yr)	1.00E+04		
Consumption Rate (m³/yr)	1.20E+00		
Dose Conversion Factor			
Isotope	**Sv/Bq**	**Isotope**	**Sv/Bq**
Ac-227	0.00E+00	Pu-242	2.40E-07
Am-241	2.00E-07	Ra-226	2.17E-06
Am-243	2.01E-07	Ra-228	0.00E+00
C-14	5.80E-10	Sb-126	0.00E+00
Cl-36	9.30E-10	Se-79	2.90E-09
Cm-245	2.15E-07	Sn-126	4.70E-09
Cs-135	2.00E-09	Sr-90	3.07E-08
Cs-137	1.30E-08	Tc-99	6.40E-10
I-129	1.10E-07	Th-229	6.13E-07
Nb-93	0.00E+00	Th-230	2.10E-07
Np-237	1.11E-07	Th-232	1.06E-06
Pa-231	1.92E-06	U-232	0.00E+00
Pb-210	0.00E+00	U-233	5.10E-08
Pd-107	3.70E-11	U-234	4.90E-08
Pu-238	2.30E-07	U-235	4.73E-08
Pu-239	2.50E-07	U-236	4.70E-08
Pu-240	2.50E-07	U-238	4.84E-08
Pu-241	0.00E+00	Zr-93	1.22E-09
Source: "Reference Biospheres for Solid Radioactive Waste Disposal," IAEA-BIOMASS-6, July 2003. Table C.5			

2.7   Fast Paths

The UFDC Clay GDSM includes the capability to represent fast paths that can be parameterized by the user to evaluate various stylized scenarios.

The far-field component of the UFDC Clay GDSM, discussed above, includes the ability to include vertical advective transport within the far field at 25%, 50%, 75%, and 100% of the domain width within the 20x20 node network. This allows for the simulation of fast paths that do not directly intersect the emplaced waste or the engineered barriers, but could degrade the isolation capability of the far field. The user is able to define the Darcy velocity in these fast paths along with a time and duration that the increased flow occurs. The input parameters are shown in Table 11.

Table 11. Far-Field Fast Path Parameters.

Position in the Far Field Domain	Velocity (m/yr)	Start Time (Year)	Duration (Years)
25%	6.31E-06		
50%	0		
75%	0	1.00E+06	2.00E+05
100%	0		

Note that the values shown are for example only.

The UFDC Clay GDSM also includes the capability to evaluate stylized scenarios of preferential fast pathways that either directly intersect the emplaced waste or the engineered barriers. This capability is shown schematically in Figure 10. The model is comprised of a diffusive and an advective radionuclide transport component. The diffusive pathway consists of a five node network of batch-reactor mixing cells to represent one-dimensional radionuclide diffusion. This diffusive pathway is linked to a two segment "pipe" network that represent one-dimensional advective-dispersive radionuclide transport between the diffusive network and the aquifer. A fast pathway scenario is defined by:

- Defining whether the fast-path network directly intersects the emplaced waste or other engineered barriers.

- Defining the distance for diffusive transport between the intersection point and the location where an advective fast-path is present;

- Defining the cross-sectional area for diffusive radionuclide transport (constant along the one-dimensional direction)

- The length and advective (Darcy) velocity in each of the two advective-dispersive segments.

The properties of the fast path are shown in Table 12 and are applied to both the diffusive and advective segment. The ability to simulate dissolution/precipitation and reversible sorption is included in each batch-reactor mixing cell for the diffusive segment. Reversible sorption is included in each advective-dispersive "pipe." The dispersivity in each advective-dispersive "pipe" is assumed to be ten-percent of the segment length. It is assumed that the dissolved concentration limits and distribution coefficients are represented in the UFDC Clay GDSM as log-triangular, as shown in Table 4, with the user having the ability to define the minimum, best estimate, and maximum values of the distribution from the input spreadsheet for the fast pathway scenario.

Table 12. Fast Path Properties.

Property	Minimum	Most Likely	Maximum
Porosity	0.15	0.20	0.25
Density (kg/m^3)	2000	2250	2500
Tortuosity	0.5	0.75	0.1

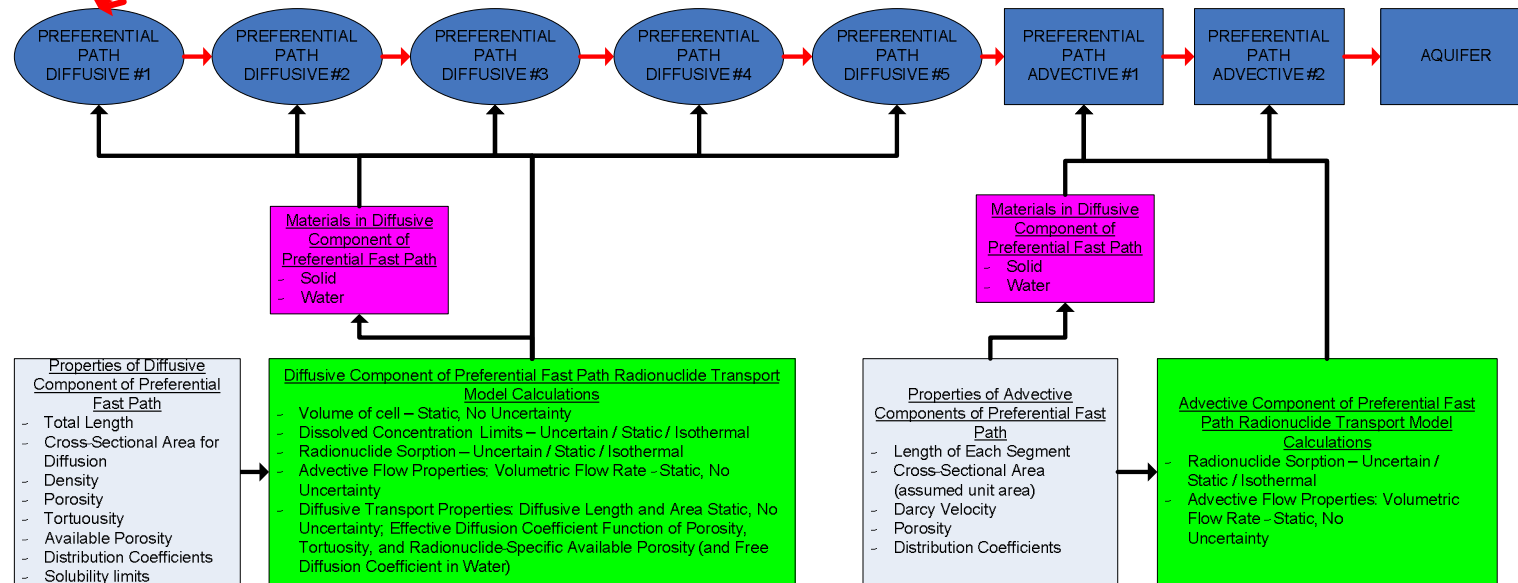Note that the values shown are for example only.

.
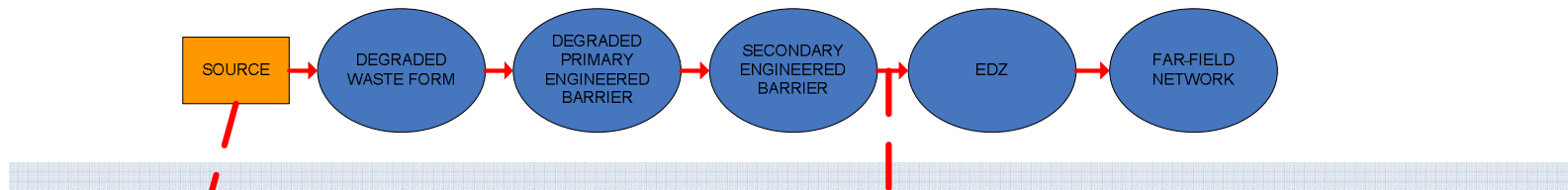
Figure 10. Schematic of Fast Pathway Simulation Capability.

The volume of each batch-reactor mixing cell is determined as:

$$V_{FP-Diffusion} = \frac{L_{FP-Diffusion}}{5} \bullet A_{FP-Diffusion}$$

Eq. 13

where

$V_{FP\text{-}Diffusion}$	=	Volume of each batch-reactor cell in the five-node diffusive network (m³)
$L_{FP\text{-}Diffusion}$	=	Length of the five-node diffusive network (m); 5 cells along the length
$A_{FP\text{-}Diffusion}$	=	Cross-sectional area for diffusive radionuclide transport (m²)

The volume of water in each batch-reactor mixing cell is equal to the product of the cell volume and the porosity. The mass of solid material in the mixing cell is equal to the product of the volume of the cell and the density (assumed to be the dry density).

The diffusive length in each cell is determined from the length of the five-node diffusive network (as $L_{FP\text{-}Diffusion}/5$).

As discussed above, the location where the preferential fast path intersects the engineered barrier system is either directly to the emplaced waste or after the secondary engineered barrier system. For the former, the entire inventory of waste is instantaneously released into the first diffusive batch-reactor mixing cell. If the later is selected, the entire "base" model is executed to determine the release rate from the secondary barrier and that mass flux exiting is input into the first diffusive batch-reactor mixing cell. For both cases, all radionuclides are assumed to be transported through the preferential fast-pathway network. This neglects any additional radionuclide transport processes that would occur along the fast pathways (i.e., transverse diffusion into the far-field) and will yield conservative results.

Two additional "fine" batch-reactor mixing cells are included before the five-node diffusive cell network. These cells are assumed to be 0.1 meters thick and are included to better capture dissolution/precipitation processes for scenarios where the preferential fast pathway directly intersects the emplaced waste.

The effective diffusion coefficient is given as:

$$D_{eff,j} = D_{ref} \bullet R_{D,j} \bullet \phi \bullet \tau \bullet \phi_{A,j}$$

Eq. 14

where

$D_{eff,j}$	=	Effective diffusion coefficient for element j (m²/yr)
D_{ref}	=	Reference diffusivity in water (m²/yr); Table 4
$R_{D,j}$	=	Relative diffusivity in water for element j; Table 4
ϕ	=	Porosity
τ	=	Tortuosity
$\phi_{A,j}$	=	Available porosity for element j (0 to 1); Table 7

This approach for determining the effective diffusion coefficient provides flexibility to the user in representing diffusive radionuclide transport in the preferential fast-pathways. As discussed above, both the reference diffusivity and the element-specific relative diffusivities are user inputs. The element-specific available porosities are represented as triangular distributions with the minimum, most likely, and maximum values being user inputs as shown in Table 7.

3.   MATERIAL PROPERTIES

Material properties, except for waste package materials are the same as used in Ref. 2 and are based on material properties used in the analysis reported in Ref. 2 for the ANDRA Dossier 2005 Argile series [Refs.5, 6, and 7]. These properties are listed and discussed in the section that follow. The engineered barrier system configuration modeled includes the waste form, the waste package, and a swelling clay secondary engineered barrier, consistent with that modeled in the ANDRA Dossier 2005 Argile safety evaluation [Ref. 7]. The ANDRA Dossier 2005 Argile safety evaluation assumed that the waste package (primary engineered barrier) failed 10,000 years following repository closure and a subsequent gradual release of radionuclides from the used nuclear fuel matrix over 50,000 years following failure of the waste package[Ref. 7, Section 5.3.2.1]. A fractional degradation rate of 2×10^{-5} yr^{-1} was therefore used in the UFDC Clay GDSM.

The waste package is assumed to have an outer diameter of 2 meters, a length of 5 meters, and a thickness of 0.0.05 meters.

The properties of the degraded waste form and primary engineered barrier used are provided in Table 13. The degraded waste form density and porosity are assumed to be that of schoepite [Ref. 11, Table 6.3.8-6], although it is recognized that schoepite may not be the resultant product of used nuclear fuel degradation in reducing conditions The volume of the waste form batch-reactor mixing cell is assumed to equal the inner volume of the waste package and the volume of the primary engineered barrier batch-reactor mixing cell is assumed to equal the volume of the waste package cylinder wall. The diffusive area for the diffusion area for the waste form and primary engineered barrier is assumed to equal the inner and outer cylinder areas, respectively, of the waste package.

Table 13. Waste Form and Primary Engineered Barrier Properties.

Property	Waste Form	Primary Engineered Barrier
Material Density (kg/m^3)	4,830	5,240
Porosity	0.175	0.4
Volume (m^3)	14.2	1.531
Thickness (m)	0.95	0.05
Diffusion Area (m^2)	29.8	31.4
Advective Flow Rate (m^3/yr)	6.31E-06	6.31E-06

The properties of the secondary engineered barrier (swelling clay) are provided in Table 14. The analyses considered a tunnel diameter of 4.5 meters. This gives a thickness of the swelling clay layer equal to 1.025 meters. The waste packages were spaced 5 m apart so that alength of 10 meters was used to determine the volume of the secondary engineered barrier batch-reactor mixing cell shown in Table 14.

No information could be found on the density or porosity of the swelling clay buffer. As such, the value of those parameters was assumed. The effective diffusion coefficients assumed in the swelling clay buffer were 5×10^{-10} m^2/s for all elements considered in the UFDC Clay GDSM, except for C, Cl, I, Nb, and Se which were 5×10^{-12} m^2/s [Ref. 7, Table 5.3-15]. For a free diffusion coefficient of 2.3×10^{-9} m^2/s (relative diffusivity of 1) and a porosity of 0.3, the tortuosity was set at 0.72 to yield the 5×10^{-10} m^2/s

effective diffusion coefficient. The available porosity was set to 0.01 for C, Cl, I, Nb, and Se to yield the effective diffusion coefficient of 5×10^{-12} m^2/s.

Table 14. Secondary Engineered Barrier Properties.

Property	Secondary Engineered Barrier
Volume (m^3)	127.6
Thickness (m)	1.25
Perimeter (m)	14.1
Advective Flow Rate (m^3/yr)	2.84E-05
Porosity	0.3
Density (kg/m^3)	2,300
Tortuosity	0.07
Fracture Spacing (m)	0.25
Fracture Aperture (m)	0.005

The advective flow rate through the swelling clay buffer (secondary engineered barrier) was assumed to equal the product of the far-field advective velocity (Darcy velocity) and the cross-sectional area (length×outer diameter) of the buffer. The far-field advective velocity is discussed below.

The dissolved concentration limits and distribution coefficients used are shown in Tables 15 and 16. As indicated by the tables, these parameters are assumed to have triangular probability distributions with the minimum and maximum values indicated. Elements for which no information source is indicated were assumed to have infinite solubility and a negligible distribution coefficient. As indicated in the tables, the minimum and maximum values for postulated triangular probability distributions were assumed to be two orders of magnitude smaller and larger, respectively, than the most likely value.

Table 15. Dissolved Concentration Limits – Swelling Clay Buffer.

Element	Mol/liter		
	Min	Most Likely	Max
Actinium	1.00E+50	1.00E+50	1.00E+50
Americium**	1.00E-12	1.00E-10	1.00E-08
Antimony	1.00E+50	1.00E+50	1.00E+50
Carbon*	2.30E-05	2.30E-03	2.30E-01
Cesium**	1.00E+50	1.00E+50	1.00E+50
Chlorine*	1.00E+50	1.00E+50	1.00E+50
Curium	1.00E+50	1.00E+50	1.00E+50
Iodine**	1.00E+50	1.00E+50	1.00E+50
Lead	1.00E+50	1.00E+50	1.00E+50
Neptunium**	4.00E-11	4.00E-09	4.00E-07
Niobium*	2.00E-09	2.00E-07	2.00E-05
Paladium*	4.00E-09	4.00E-07	4.00E-05
Protactinium	1.00E+50	1.00E+50	1.00E+50
Plutonium**	1.99E-09	1.99E-07	1.99E-05
Radium	1.00E+50	1.00E+50	1.00E+50
Selenium*	5.00E-12	5.00E-10	5.00E-08
Strontium	1.00E+50	1.00E+50	1.00E+50
Technitium*	4.00E-11	4.00E-09	4.00E-07
Thorium**	1.00E-11	1.00E-09	1.00E-07
Tin*	1.00E-10	1.00E-08	1.00E-06
Uranium**	5.00E-10	5.00E-08	5.00E-06
Zirconium*	2.00E-10	2.00E-08	2.00E-06

* Most likely value from Ref. 7

** Most likely value from Ref. 6

Table 16. Distribution Coefficients – Swelling Clay Buffer.

Element	m³/kg		
	Min	Most Likely	Max
Actinium	1.00E-51	1.00E-50	1.00E-49
Americium**	1.20E-01	1.20E+01	1.20E+03
Antimony	1.00E-51	1.00E-50	1.00E-49
Carbon*	9.99E-51	1.00E-50	1.00E-50
Cesium*	4.37E-04	4.37E-02	4.37E+00
Chlorine*	9.99E-51	1.00E-50	1.00E-50
Curium	1.00E-51	1.00E-50	1.00E-49
Iodine*	9.99E-51	1.00E-50	1.00E-50
Lead	1.00E-51	1.00E-50	1.00E-49
Neptunium**	1.00E-02	1.00E+00	1.00E+02
Niobium*	3.15E-01	3.15E+01	3.15E+03
Paladium*	3.94E-03	3.94E-01	3.94E+01
Protactinium	1.00E-51	1.00E-50	1.00E-49
Plutonium**	1.00E-02	1.00E+00	1.00E+02
Radium	9.99E-51	1.00E-50	1.00E-50
Selenium**	1.00E-05	1.00E-03	1.00E-01
Strontium	1.00E-51	1.00E-50	1.00E-49
Technitium*	1.31E-01	1.31E+01	1.31E+03
Thorium**	3.00E-02	3.00E+00	3.00E+02
Tin*	4.81E+00	4.81E+00	4.81E+02
Uranium**	1.00E+00	1.00E+02	1.00E+04
Zirconium*	4.37E+01	4.37E+01	4.37E+03

* Most likely value from Ref. 7
** Most likely value from Ref. 6

The evolution of the EDZ is described in the Dossier 2005 Argile, *Phenomenological Evolution of a Geologic Repository* report [Ref. 6, Section 8.2.3]. The EDZ consists of a fractured zone in the immediate vicinity of the engineered structure and a microfissured zone behind the fractured zone. In a repository 500 meters deep, ANDRA states that the fractured zone will extend for 15 centimeters and the microfracture zone will extend for over one meter. The UFDC Clay GDSM representation assumes an EDZ thickness of 1.15 meters.

The properties of the EDZ are provided in Table 17. The outer diameter of the EDZ was assumed to be 6.8 m and its length equal to the waste package length plus the waste package separation distance, a value of 10 m. Other parameters were assumed to be the same as the corresponding values for the far field.

The effective diffusion coefficients assumed in the EDZ were 2.5×10^{-10} m²/s for all elements considered in the UFDC Clay GDSM with the exception that the values for C, Cl, I, Nb, and Se were assumed to be 5×10^{-12} m²/s [Ref. 7, Table 5.3-14]. For a free diffusion coefficient of 2.3×10^{-9} m²/s (relative diffusivity of 1) and a porosity of 0.18, the tortuosity was set at 0.6 to yield the 2.5×10^{-10} m²/s effective diffusion coefficient. The available porosity was set to 0.02 for C, Cl, I, Nb, and Se to yield the effective diffusion coefficient of 5×10^{-12} m²/s.

The advective flow rate through the EDZ was assumed to equal the product of the far-field advective velocity (Darcy velocity) and the cross-sectional area (length×outer diameter) of the EDZ. The far-field advective velocity is discussed below.

The dissolved concentration limits and distribution coefficients used are shown in Tables 18 and 19.

The properties of the far-field are shown in Table 20. The advective velocity through the far-field was 6.31×10^{-7} m/yr, based on a vertical hydraulic gradient of 5.0×10^{-14} m/s and a vertical hydraulic gradient of 0.4 [Ref. 7, Table 5.5-1]. The dissolved concentration limits and distribution coefficients used are shown in Tables 21 and 22. The depth of the far field from the repository horizon to the aquifer above the repository is assumed to be 65 m.

Table 17. EDZ Properties – ANDRA Benchmark.

Property	Excavation Damage Zone
Volume (m^3)	204.1
Thickness (m)	1.15
Perimeter (m)	21.4
Advective Flow Rate (m^3/yr)	4.29E-05
Porosity	0.18
Density (kg/m^3)	2000
Tortuosity	0.06
Fracture Spacing (m)	0.5
Fracture Aperture (m)	0.001

Note that while the UFDC Clay GDSM was used in deterministic mode to conduct the ANDRA Dossier 2005 Argile benchmark

Table 18. Dissolved Concentration Limits for the EDZ.

Element	Mol/liter		
	Min	Most Likely	Max
Actinium	4.00E-09	4.00E-07	4.00E-05
Americium	4.00E-09	4.00E-07	4.00E-05
Antimony*	1.00E+50	1.00E+50	1.00E+50
Carbon	2.30E-05	2.30E-03	2.30E-01
Cesium	1.00E+50	1.00E+50	1.00E+50
Chlorine	1.00E+50	1.00E+50	1.00E+50
Curium	4.00E-09	4.00E-07	4.00E-05
Iodine	1.00E+50	1.00E+50	1.00E+50
Lead	4.00E-08	4.00E-06	4.00E-04
Neptunium	4.00E-11	4.00E-09	4.00E-07
Niobium	2.00E-09	2.00E-07	2.00E-05
Paladium	4.00E-09	4.00E-07	4.00E-05
Protactinium	1.00E-08	1.00E-06	1.00E-04
Plutonium	2.00E-09	2.00E-07	2.00E-05
Radium	1.00E-09	1.00E-07	1.00E-05
Selenium	5.00E-12	5.00E-10	5.00E-08
Strontium*	1.00E+50	1.00E+50	1.00E+50
Technitium	4.00E-11	4.00E-09	4.00E-07
Thorium	6.00E-09	6.00E-07	6.00E-05
Tin	1.00E-10	1.00E-08	1.00E-06
Uranium	7.00E-09	7.00E-07	7.00E-05
Zirconium	2.00E-10	2.00E-08	2.00E-06

* Assume infinite solubility since no information is available

Table 19. Distribution coefficients for the EDZ.

Element	m^3/kg		
	Min	Most Likely	Max
Actinium	5.00E-01	5.00E+01	5.00E+03
Americium	5.00E-01	5.00E+01	5.00E+03
Antimony*	1.00E-51	1.00E-50	1.00E-49
Carbon	4.14E-06	4.14E-04	4.14E-02
Cesium	4.00E-03	4.00E-01	4.00E+01
Chlorine	1.00E-51	1.00E-50	1.00E-49
Curium	5.00E-01	5.00E+01	5.00E+03
Iodine	1.00E-51	1.00E-50	1.00E-49
Lead	1.60E-03	1.60E-01	1.60E+01
Neptunium	9.00E-03	9.00E-01	9.00E+01
Niobium	4.81E-02	4.81E+00	4.81E+02
Paladium	8.05E-03	8.05E-01	8.05E+01
Protactinium	1.00E-02	1.00E+00	1.00E+02
Plutonium	9.00E-03	9.00E-01	9.00E+01
Radium	1.00E-02	1.00E+00	1.00E+02
Selenium	9.99E-51	1.00E-50	1.00E-50
Strontium*	9.99E-51	1.00E-50	1.00E-50
Technitium	1.15E-02	1.15E+00	1.15E+02
Thorium	8.00E-02	8.00E+00	8.00E+02
Tin	1.61E-01	1.61E+01	1.61E+03
Uranium	8.00E-02	8.00E+00	8.00E+02
Zirconium	1.15E-02	1.15E+00	1.15E+02

* Assume negligible since no information is available

Table 20. Far Field Properties

Property	Value
Porosity	0.18
Density (kg/m^3)	2,000
Tortuosity : X-dimension	0.06
Tortuosity : Y-dimension	0.06

Note that while the UFDC Clay GDSM was used in deterministic mode to conduct the ANDRA Dossier 2005 Argile benchmark

Table 21. Dissolved Concentration Limits – Far-Field.

Element	Mol/liter		
	Min	Most Likely	Max
Actinium	4.00E-09	4.00E-07	4.00E-05
Americium	4.00E-09	4.00E-07	4.00E-05
Antimony*	1.00E+50	1.00E+50	1.00E+50
Carbon	2.30E-05	2.30E-03	2.30E-01
Cesium	1.00E+50	1.00E+50	1.00E+50
Chlorine	1.00E+50	1.00E+50	1.00E+50
Curium	4.00E-09	4.00E-07	4.00E-05
Iodine	1.00E+50	1.00E+50	1.00E+50
Lead	4.00E-08	4.00E-06	4.00E-04
Neptunium	4.00E-11	4.00E-09	4.00E-07
Niobium	2.00E-09	2.00E-07	2.00E-05
Paladium	4.00E-09	4.00E-07	4.00E-05
Protactinium	1.00E-08	1.00E-06	1.00E-04
Plutonium	2.00E-09	2.00E-07	2.00E-05
Radium	1.00E-09	1.00E-07	1.00E-05
Selenium	5.00E-12	5.00E-10	5.00E-08
Strontium*	1.00E+50	1.00E+50	1.00E+50
Technitium	4.00E-11	4.00E-09	4.00E-07
Thorium	6.00E-09	6.00E-07	6.00E-05
Tin	1.00E-10	1.00E-08	1.00E-06
Uranium	7.00E-09	7.00E-07	7.00E-05
Zirconium	2.00E-10	2.00E-08	2.00E-06

* Assume infinite solubility since no information is available

Table 22. Distribution Coefficients – Far-Field.

Element	m^3/kg		
	Min	Most Likely	Max
Actinium	5.00E-01	5.00E+01	5.00E+03
Americium	5.00E-01	5.00E+01	5.00E+03
Antimony*	1.00E-51	1.00E-50	1.00E-49
Carbon	4.14E-06	4.14E-04	4.14E-02
Cesium	4.00E-03	4.00E-01	4.00E+01
Chlorine	1.00E-51	1.00E-50	1.00E-49
Curium	5.00E-01	5.00E+01	5.00E+03
Iodine	1.00E-51	1.00E-50	1.00E-49
Lead	1.60E-03	1.60E-01	1.60E+01
Neptunium	9.00E-03	9.00E-01	9.00E+01
Niobium	4.81E-02	4.81E+00	4.81E+02
Paladium	8.05E-03	8.05E-01	8.05E+01
Protactinium	1.00E-02	1.00E+00	1.00E+02
Plutonium	9.00E-03	9.00E-01	9.00E+01
Radium	1.00E-02	1.00E+00	1.00E+02
Selenium	9.99E-51	1.00E-50	1.00E-50
Strontium*	1.00E-51	1.00E-50	1.00E-50
Technitium	1.15E-02	1.15E+00	1.15E+02
Thorium	8.00E-02	8.00E+00	8.00E+02
Tin	1.61E-01	1.61E+01	1.61E+03
Uranium	8.00E-02	8.00E+00	8.00E+02
Zirconium	1.15E-02	1.15E+00	1.15E+02

* Assume negligible since no information is available

4.   CALCULATIONS FOR 32-PWR WASTE PACKAGE

In Ref. 2 calculations were presented for a hypothetical repository containing waste packages each containing 4 PWR fuel assemblies. Based on thermal considerations, it was found that for waste package drifts would need to be spaced approximately 5.5 m apart. For waste packages containing 32 PWR fuel assemblies, calculations are shown in Ref. 12 for drift spacings ranging from 30 m up to 70 m. The lowest peak rock wall temperature in these calculations was 119 °C for a drift spacing of 70 m. Based on visual extrapolation of the results one can estimate that the peak rock wall temperature would be close to 100 °C for a drift spacing of 90 m. This drift spacing was adopted for the calculation to be described in this section.

4.1   Reference Results

The reference calculation was carried out for an radioisotope inventory consisting of PWR fuel with a burnup of 60 GWd/MT and cooled 30 years before placement in the repository. Isotopic masses for this case are listed as Inventory 1 in Table 23. Figure 11 shows the mean, median, and several percentiles for the annual dose. The results have been normalized to correspond to a repository containing one metric ton of spent fuel. The plot shows that the ten million year time frame is sufficient to capture the peak dose. Figure 24 shows the contribution of several isotopes to the dose. The figure shows that the dominant contributor to the dose is ^{129}I. The next most important contributors are ^{36}Cl and ^{135}Cs, however, the contribution from each of these isotopes is more than three orders of magnitude lower than the peak contribution from ^{129}I. Figure 12 also shows that while the ten million year time period is sufficient to capture the peak total dose, several isotopes have their peak contribution beyond this time frame. The curves in Figure 13 show the estimated probability of exceeding a given peak annual dose at 100,000, 1,000,000, and 10,000,000 years. While a detailed comparison has not been made with the results reported in Ref. 2, the results shown in Figures. 11, 12, and 13 are very similar to the previous results both in terms of the magnitude of the peak dose and in terms of the relative importance of various isotopic contributions to the dose.

Table 23. Inventories (g/WP) for Fuels With Various Burnups and Cooling Periods.

Isotope	Inventory 1	Inventory 2	Inventory 3	Inventory 4	Inventory 5	Inventory 6
Ac227	6.33E-06	1.73E-06	1.25E-05	3.46E-05	4.35E-06	1.92E-06
Am241	2.00E+04	6.56E+03	2.34E+04	1.24E+04	1.87E+04	1.16E+04
Am243	4.33E+03	4.34E+03	4.30E+03	4.14E+03	2.21E+03	4.78E+02
C14	7.26E+00	7.28E+00	7.20E+00	6.86E+00	4.98E+00	3.17E+00
Cl36	8.02E+00	8.02E+00	8.02E+00	8.02E+00	5.63E+00	3.76E+00
Cm245	1.53E+02	1.53E+02	1.52E+02	1.47E+02	3.79E+01	2.16E+00
Cs135	1.23E+04	1.24E+04	1.24E+04	1.23E+04	7.78E+03	3.02E+03
Cs137	1.67E+04	2.98E+04	3.31E+03	3.22E-01	1.14E+04	5.84E+03
I129	5.01E+03	5.01E+03	5.01E+03	5.01E+03	3.46E+03	1.76E+03
Nb93	1.14E+04	1.14E+04	1.14E+04	1.14E+04	1.15E+04	1.16E+04
Np237	1.98E+04	1.92E+04	2.24E+04	3.33E+04	1.15E+04	4.10E+03
Pa231	1.64E-02	1.43E-02	2.22E-02	5.55E-02	1.23E-02	6.59E-03
Pb210	1.80E-07	8.64E-09	4.40E-06	2.90E-04	1.54E-07	1.07E-07
Pd107	6.60E+03	6.61E+03	6.61E+03	6.61E+03	4.30E+03	2.02E+03
Pu238	7.87E+03	9.58E+03	4.54E+03	1.97E+02	3.36E+03	6.69E+02
Pu239	1.19E+05	1.19E+05	1.18E+05	1.17E+05	1.02E+05	7.50E+04
Pu240	6.55E+04	6.43E+04	6.58E+04	6.30E+04	4.11E+04	2.32E+04
Pu241	6.04E+03	2.02E+04	2.08E+02	2.45E-01	5.68E+03	3.60E+03
Pu242	1.31E+04	1.31E+04	1.31E+04	1.31E+04	9.04E+03	3.65E+03
Ra226	5.09E-05	3.97E-06	6.38E-04	2.59E-02	4.40E-05	3.17E-05
Ra228	3.30E-11	4.06E-12	1.28E-10	6.96E-10	2.37E-11	1.22E-11
Sb126	3.80E-05	3.79E-05	3.79E-05	3.78E-05	2.54E-05	1.26E-05
Se79	1.68E+02	1.68E+02	1.68E+02	1.66E+02	1.13E+02	5.76E+01
Sn126	7.99E+02	7.98E+02	7.98E+02	7.97E+02	5.34E+02	2.66E+02
Sr90	7.10E+03	1.29E+04	1.34E+03	9.84E-02	4.93E+03	2.61E+03
Tc99	2.04E+04	2.05E+04	2.05E+04	2.05E+04	1.47E+04	7.84E+03
Th229	1.02E-04	8.66E-05	2.37E-04	4.27E-03	3.14E-05	5.70E-06
Th230	3.65E-01	8.13E-02	1.66E+00	1.42E+01	3.10E-01	2.29E-01
Th232	9.77E-02	2.51E-02	3.02E-01	1.49E+00	7.10E-02	3.73E-02
U232	7.29E-02	7.39E-02	3.71E-02	7.92E-04	2.98E-02	5.34E-03
U233	2.24E-01	6.88E-02	6.93E-01	4.30E+00	1.36E-01	5.06E-02
U234	4.89E+03	3.20E+03	8.18E+03	1.25E+04	3.78E+03	2.67E+03
U235	8.60E+04	8.59E+04	8.62E+04	8.75E+04	1.34E+05	1.50E+05
U236	9.99E+04	9.97E+04	1.00E+05	1.03E+05	7.54E+04	4.11E+04
U238	1.46E+07	1.46E+07	1.46E+07	1.46E+07	1.49E+07	1.54E+07
Zr93	2.35E+04	2.35E+04	2.35E+04	2.35E+04	1.60E+04	8.30E+03

Inventory 1: Burnup 60 GWD/MT, 30 -year cooled
Inventory 2: Burnup 60 GWD/MT, 5 -year cooled
Inventory 3: 60 GWD/MT, 100 -year cooled
Inventory 4: Burnup 60 GWD/MT, 500 -year cooled
Inventory 5: Burnup 40 GWD/MT, 30 -year cooled
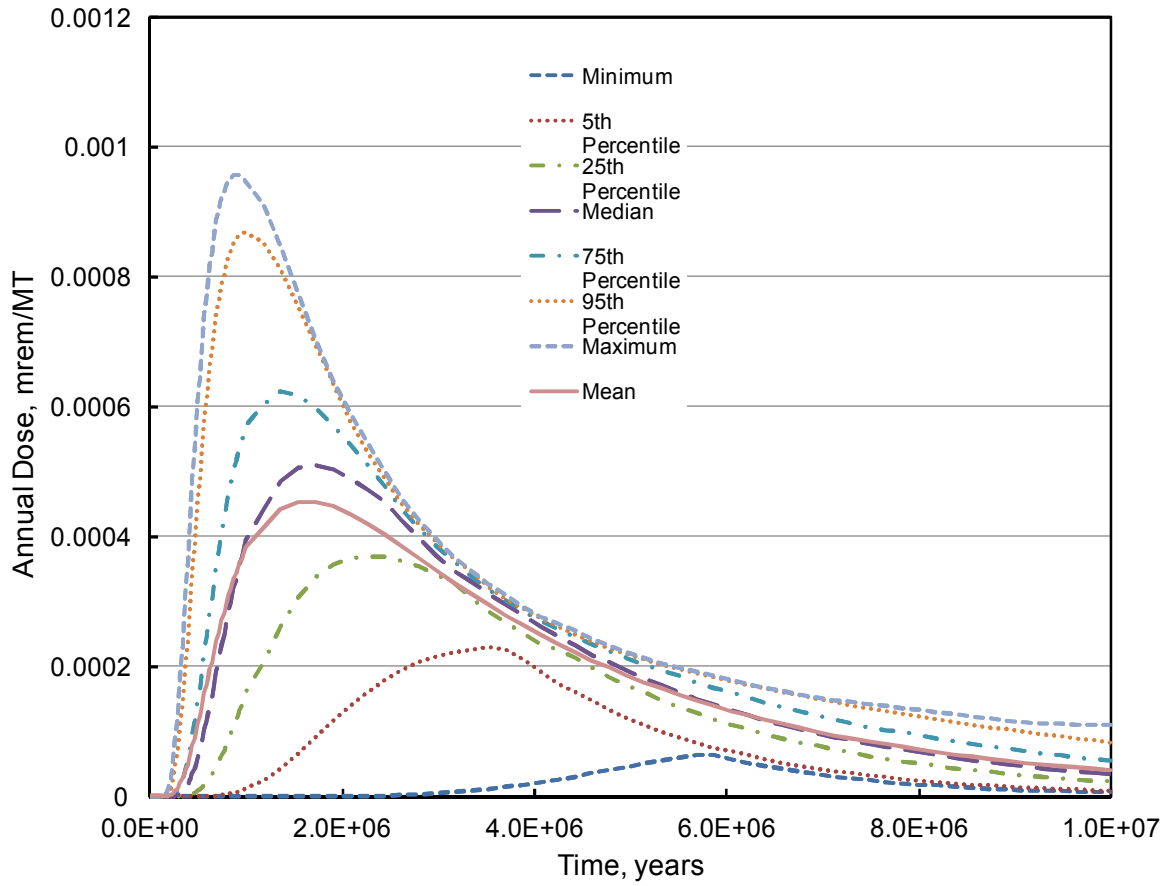Inventory 6: Burnup 20 GWD/MT, 30 -year cooled
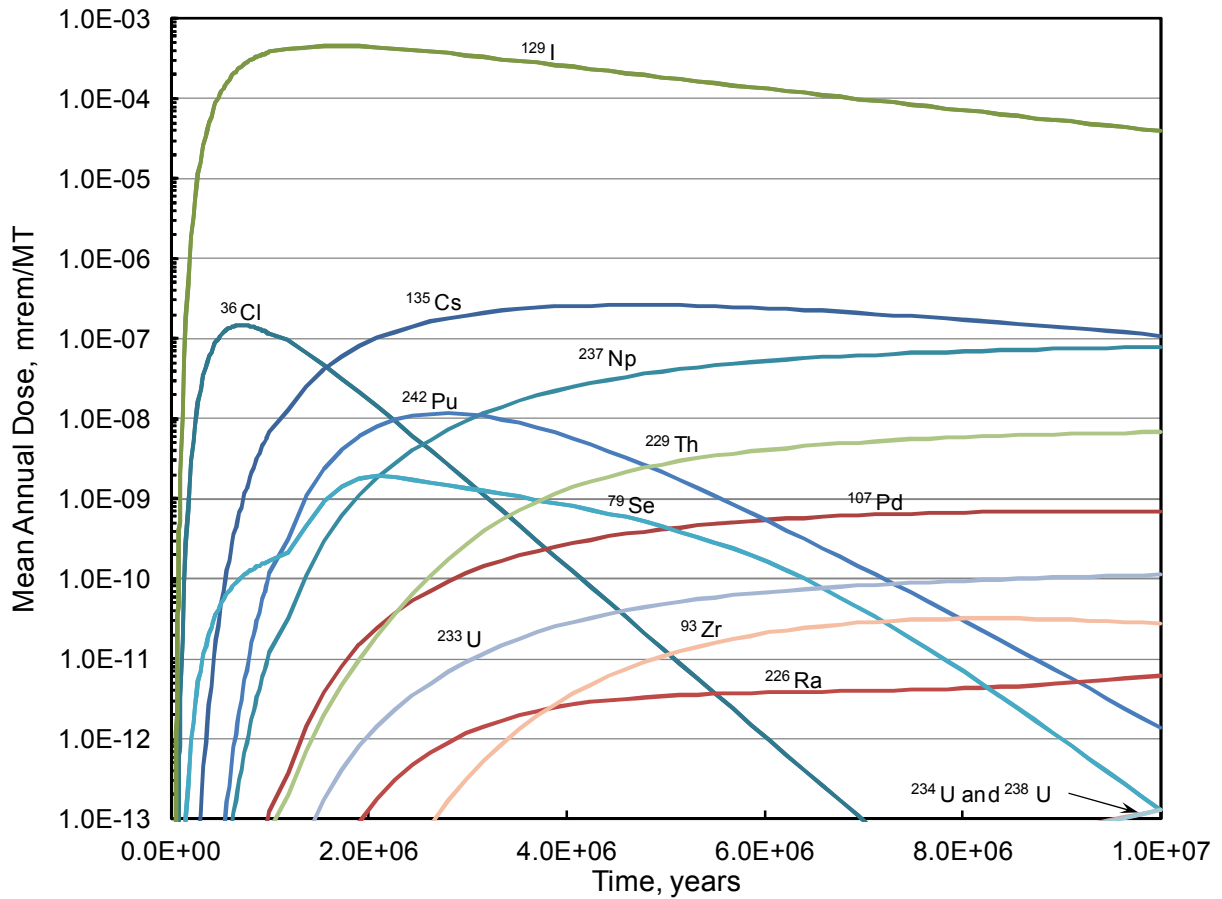
Figure 11. Time History of Total Annual Dose.

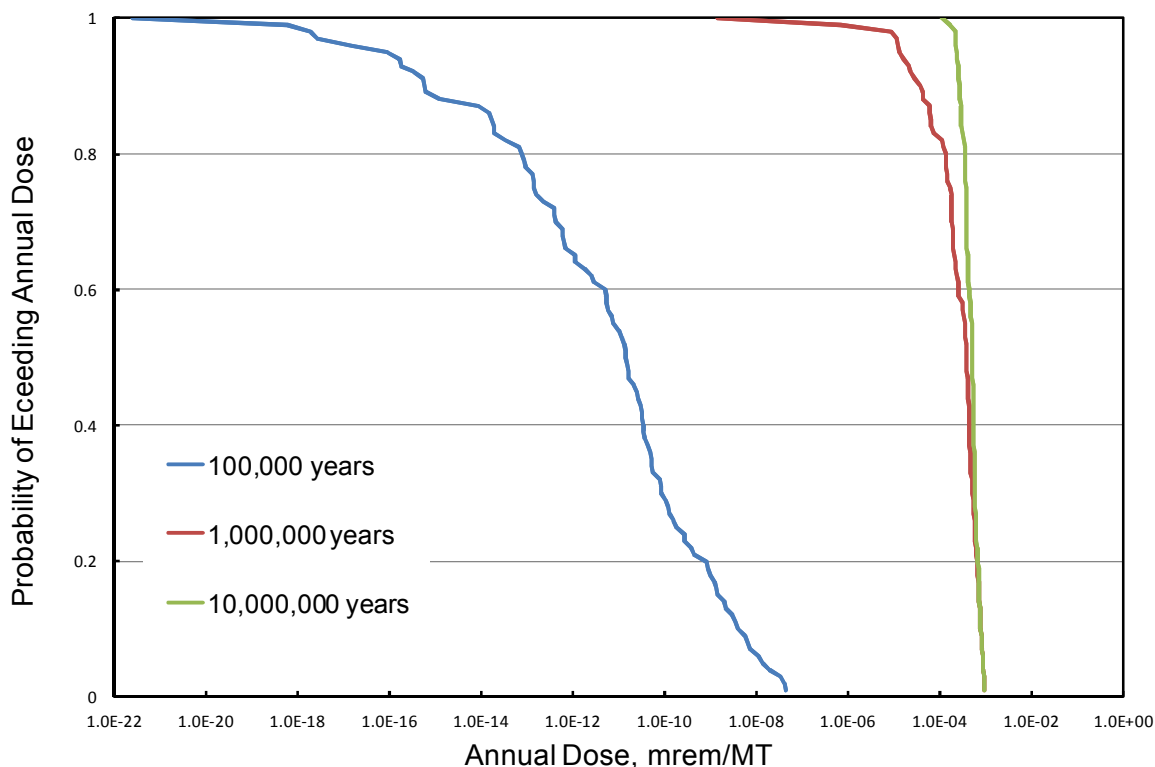Figure 12. Radionuclide Contribution to the Mean Total Annual Dose.

Figure 13. Distribution of Total Annual Dose.

4.2   Sensitivity Analysis

As was done in Ref. 2, a limited number of sensitivity analyses were conducted. These sensitivity analyses were carried out with 100 realizations varying select parameter values as discussed below. Two groups of sensitivity analyses were conducted. The first considers the "nominal" disposal system and the second considers stylized hypothetical fast radionuclide transport pathway scenarios.

4.2.1   Nominal Sensitivity Analyses

The first sensitivity considers the effect of the time between reactor discharge of the used nuclear fuel and when it is directly disposed of in the repository for pressurized water reactor (PWR) used nuclear fuel with a burn-up of 60 GWd/MT. Times from 5 to 500 years were considered. Inventories for cooling times of 5, 100, and 500 years are listed as inventories 2, 3, and 4 in Table 23. The results are shown in Figure 14. No sensitivity is seen. This is due to [129]I with a half-life of 1.6 million years, being the dominant radionuclide and decaying very little up to 500 years following reactor discharge.

For the second sensitivity study, the burnup was varied while holding the cooling time constant at 30 years. Figure 27 shows that the annual peak dose is a linear function of the burnup. Radionuclide inventories for burnups of 20 and 40 GWd/MT are listed as inventories 5 and 6 in Table 23 The linear behavior results because the dominant contributor to the dose, [129]I, has a small absorption cross section and its production is directly proportional to burnup.

The third sensitivity study, shown in Figure 16, evaluated the dependence of the peak annual dose on the waste form fractional degradation rate for PWR used nuclear fuel with a burnup of 60 GWd/MT ,

disposed of 30 years following reactor discharge. The results show that the performance of the waste form becomes more important as the fractional degradation rate decreases (waste form lifetime increases). At waste form degradation rates in the vicinity of 10^{-5} yr^{-1}, virtually all the waste form inventory is released to the far field within a few hundred thousand years. Further increases in the degradation rate may release the inventory earlier but it cannot result in a larger peak dose in the biosphere. As the waste form degradation rate decreases, a smaller and smaller fraction of the waste form inventory is released within several hundred thousand or a few million years and the dose rate to the biosphere begins to decrease.
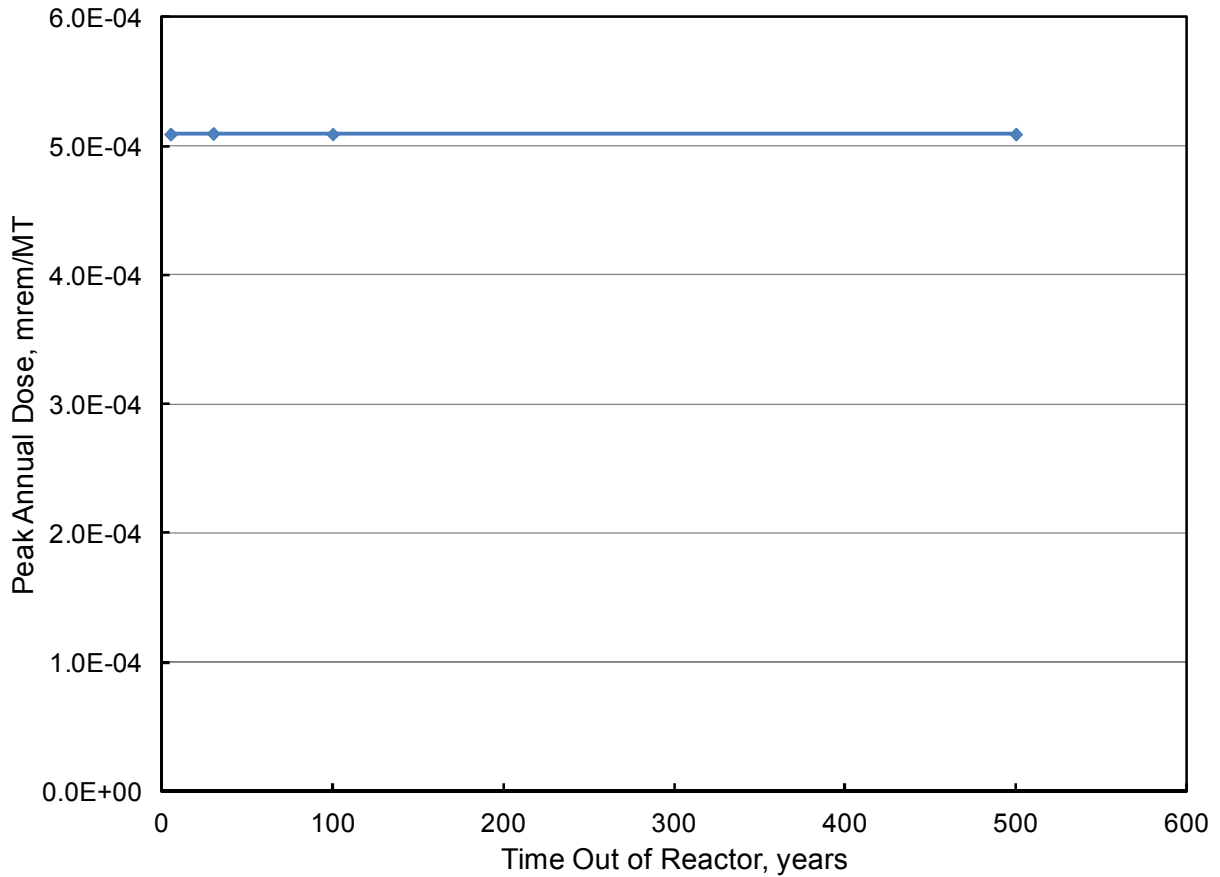
Figure 14. Sensitivity Analysis – Effect of Used Nuclear Fuel Decay for Fuel with Burnup of 60 GWd/MT.
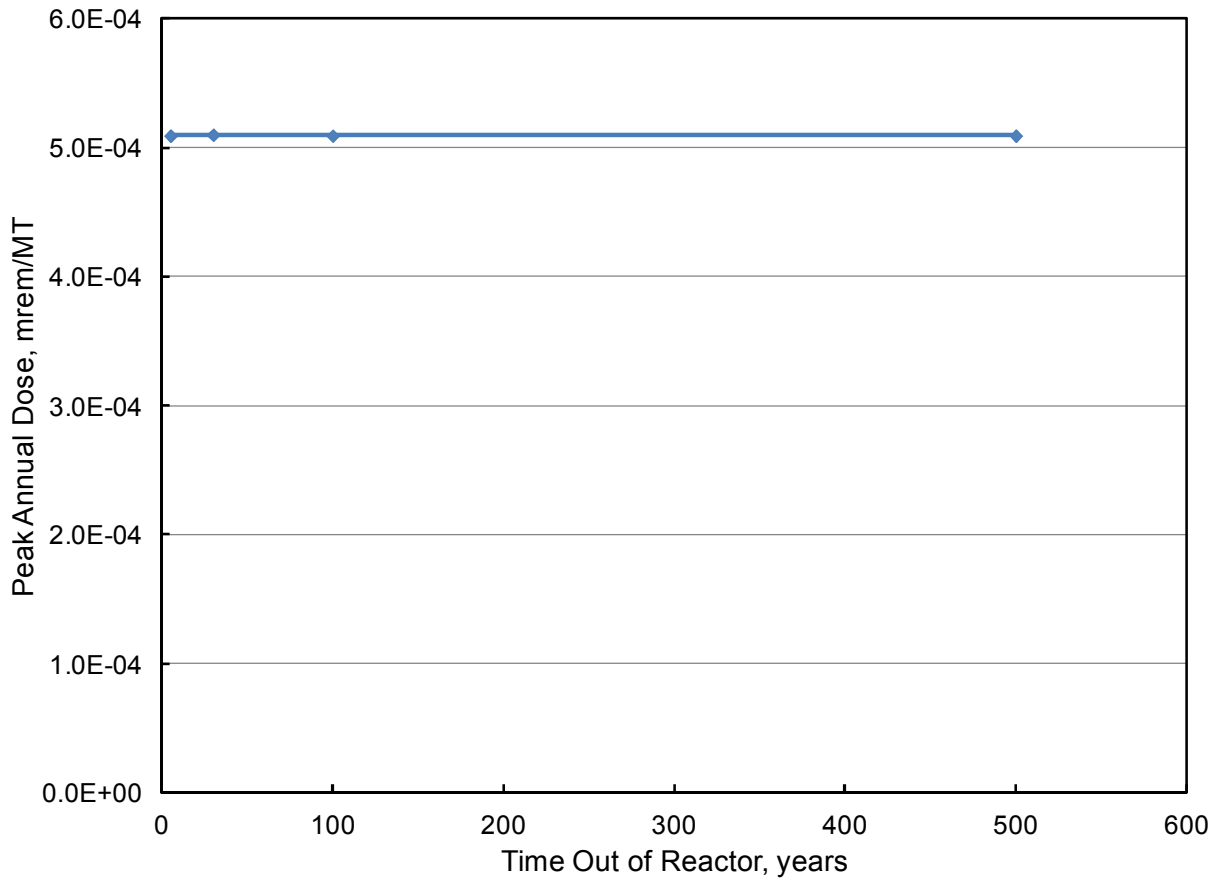
Figure 15. Dependence of the Peak Annual Dose on Burnup.
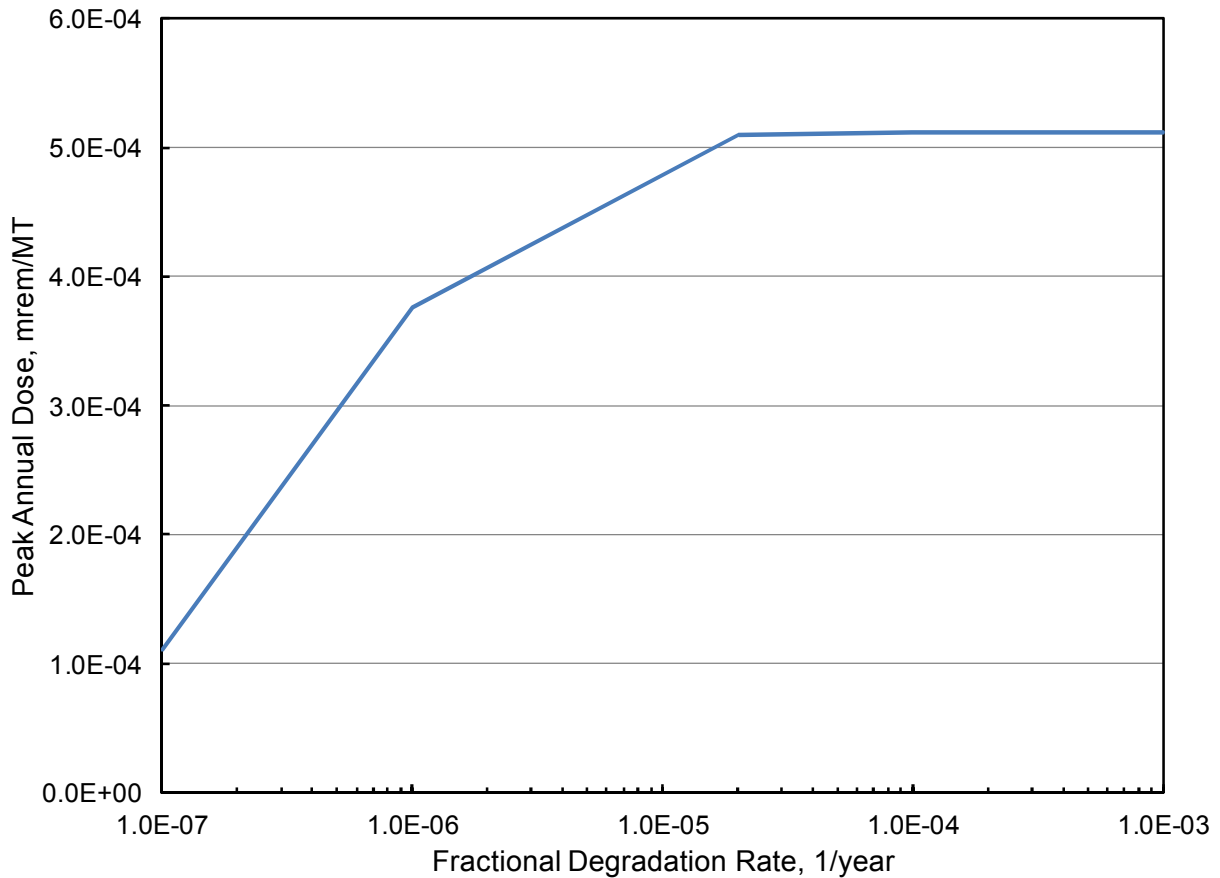
Figure 16. Effect Fractional Degradation Rate for Fuel with 60 GWd/MT Burnup and 30-years out of Reactor.

At very low waste form degradation rates (approaching 1 to 10 million year waste form lifetimes), the release from the waste form controls the release rate from the entire disposal system.

A fourth sensitivity analysis explores the effect of disposal system configuration. Figure 17 show the dependence of the peak annual dose on the domain width (half the drift spacing distance). The graph show that increasing or decreasing the separation distance between drifts by as much as a factor of two changes the peak annual dose by no more than 2%. In Figure 18, the peak annual dose is shown as a function of the distance between the repository horizon and the aquifer. The results show strong sensitivity to the distance to an overlying aquifer.

The fifth sensitivity analysis evaluated the effects of increasing the vertical advective velocity (Darcy velocity) in the far field. The results, provided in Figure 19, show that the peak annual dose is nearly a linear function of the Darcy velocity.
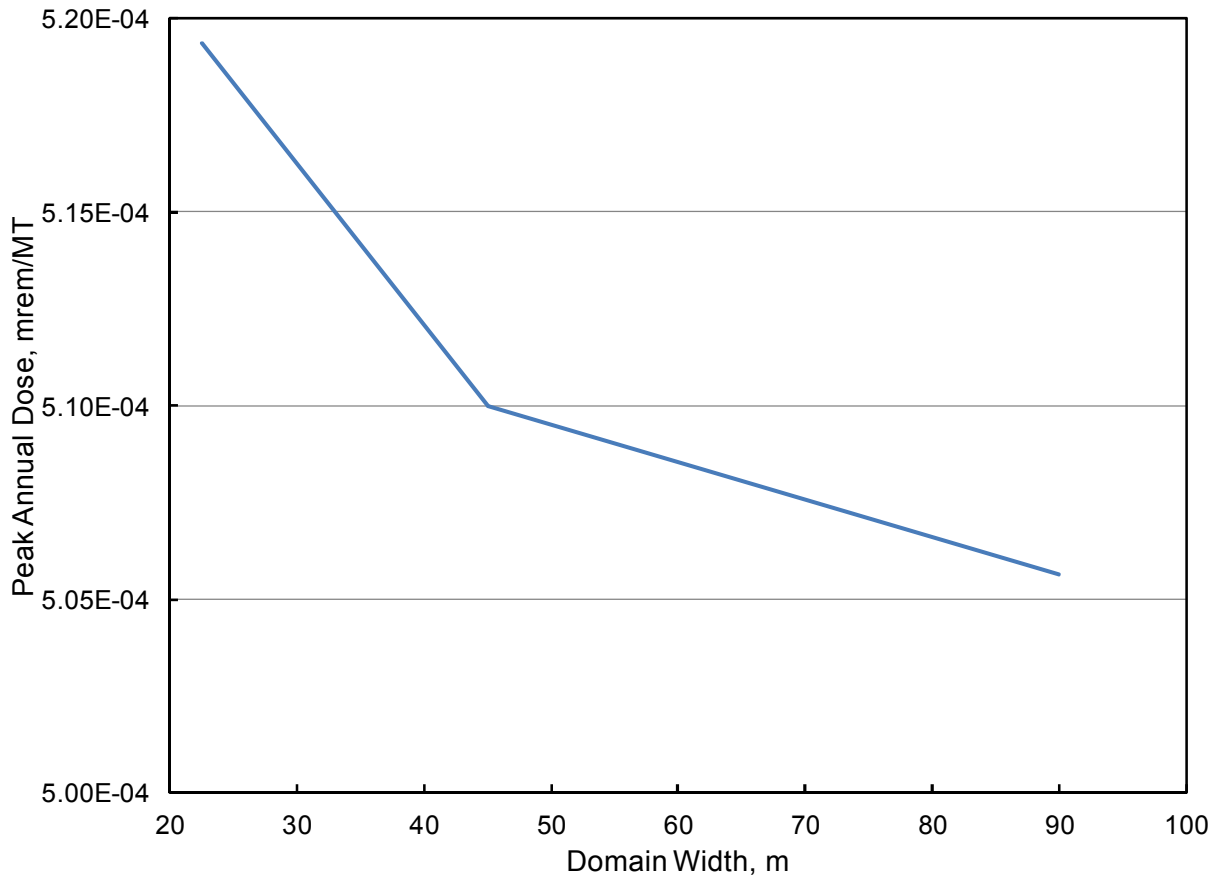
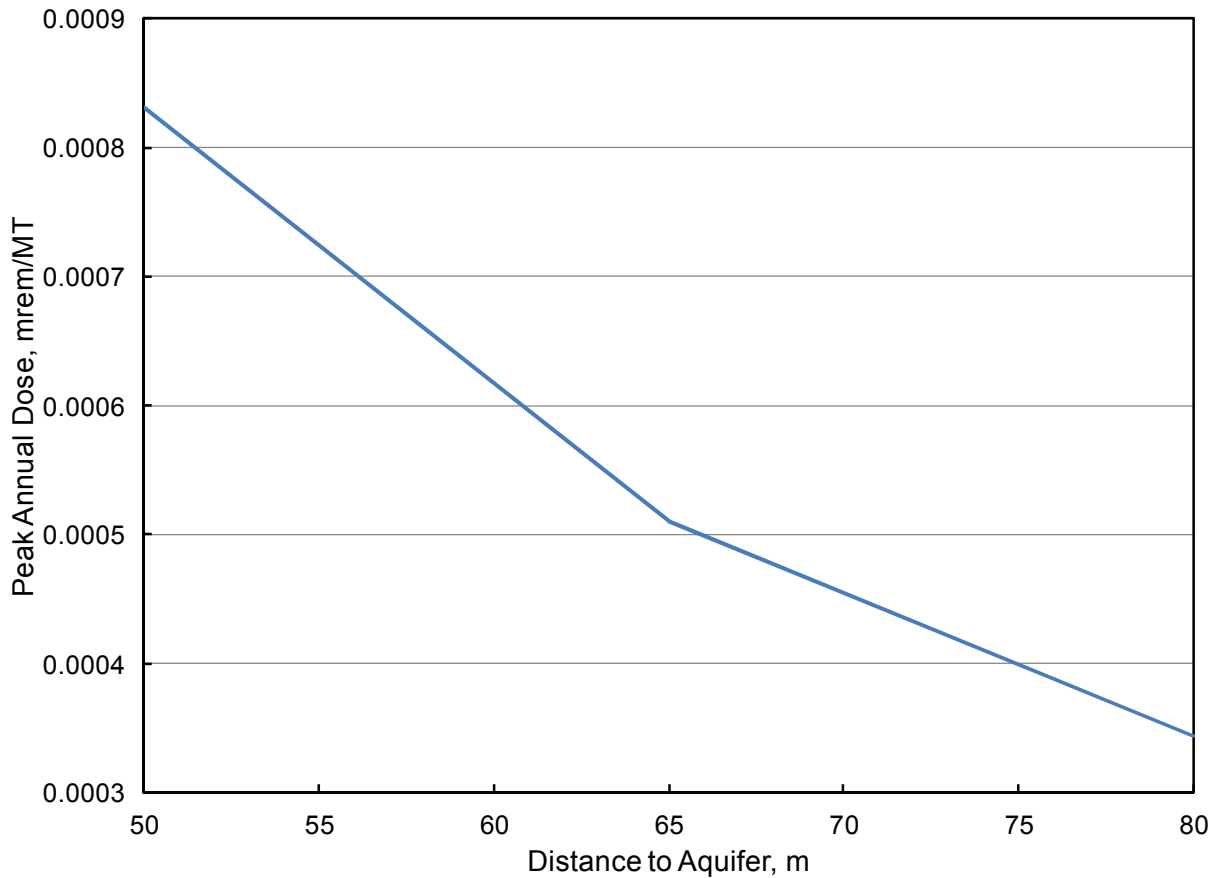Figure 17. Peak Annual Dose as a Function of the Domain Width.

Figure 18. Peak Annual Dose as a Function of the Distance from the Repository Horizon to the Aquifer.

4.2.2   Hypothetical, Fast Pathway Sensitivity Analyses

The first hypothetical fast pathway analysis considered episodic advective pathways through the far-field, first located 25 percent of the distance between the emplaced waste and the mid-plane between waste emplacement locations and second at 100% of this distance. The vertical ground water velocity (Darcy velocity) was assumed to flow episodically starting at 1,000,000 years and continuing for 500,000 years at varying rates. The results are shown in Figure 20. A significant sensitivity is seen only when the vertical groundwater velocity exceeds 100 times the "baseline" groundwater velocity (6.3×10^{-7} m/yr). Not surprisingly, the effectiveness of the episodic flow decreases as the distance of the fast path from the waste emplacement increases.
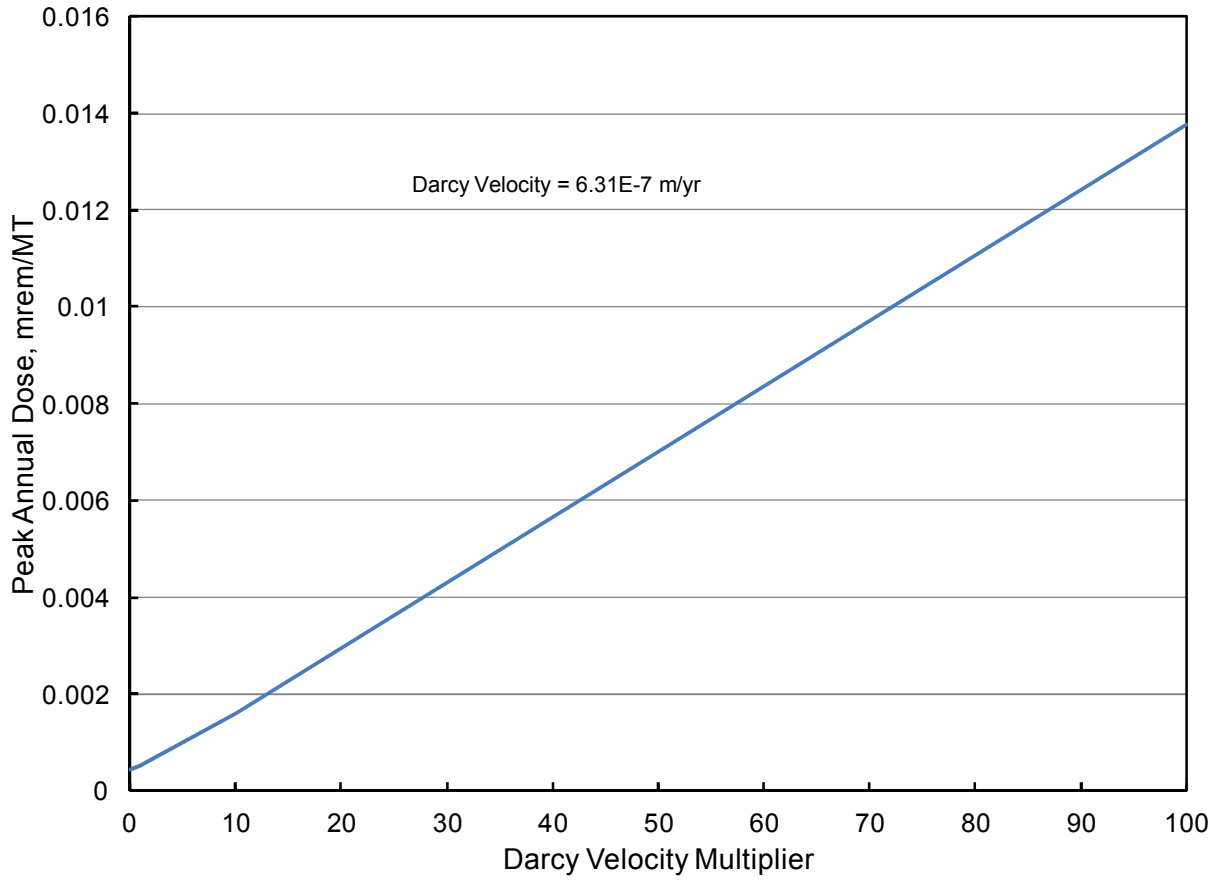
Figure 19. Peak Annual Dose as Function of the Far-Field Darcy Velocity Multiplier.
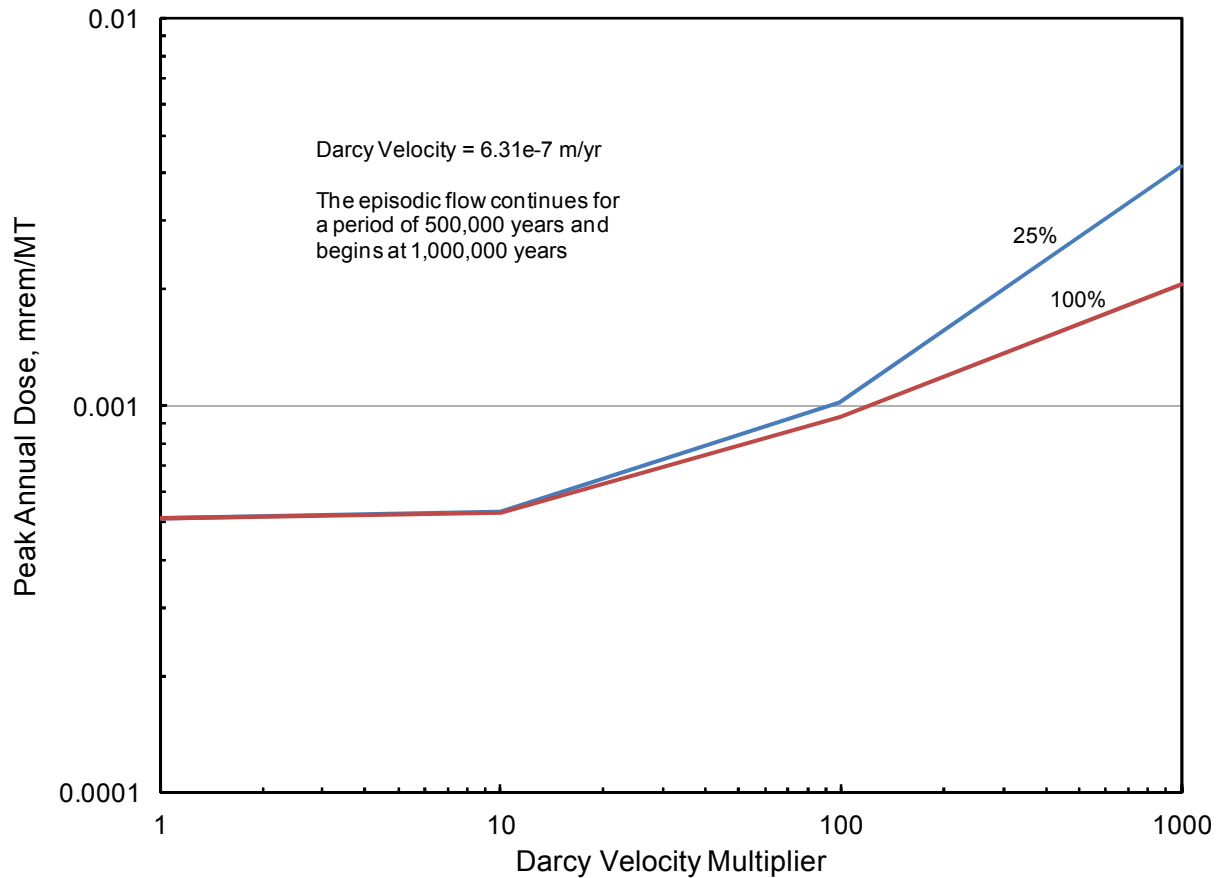
Figure 20. Impact of Episodic Far-Field Advective Transport Fast Pathway.

The second hypothetical fast pathway analysis considered an advective pathway directly intersecting the emplaced waste. No performance capability is ascribed to any engineered barriers and the radionuclide transport is assumed to occur via advective transport along a 65 meter pathway to the overlying aquifer. Distribution coefficients for the pathway were assumed to be the same as for the far field. The vertical groundwater velocity (Darcy velocity) was assumed to 0.001 m/yr. The annual dose for this case is shown in Figure 21 and is large compared to the doses in other cases considered in this report. Figure 22 shows the contribution of several isotopes to the mean annual dose. Because [129]I is non-sorbing it is the dominant contributor to the peak dose and is the most rapidly released to the environment. Late in the transient, the dose is dominated by sorbing radionuclides such as [135]Cs and [242]Pu. The third hypothetical fast pathway analysis built on that immediately above and included a 10-meter diffusive pathway between the emplaced waste and the advective fast pathway. The cross-section for diffusion was assumed to equal 5 m[2]. The properties of this diffusive zone were assumed to be identical to those of the EDZ discussed above. The free diffusion coefficient was increased by an order of magnitude, leading to a 10-fold increase in the effective diffusion coefficient in this diffusive zone as compared to that of the EDZ discussed above. Results for the mean and various percentiles are shown in Figure 23. The peak mean annual dose for this hypothetical scenario was essentially the same as in the previous case, however, doses near the peak value were confined to a shorter time period. Important isotopic contributors to the dose are the same as in the previous case with more strongly sorbing elements, including actinides such as Pu and Np, contributing significantly only at later times.
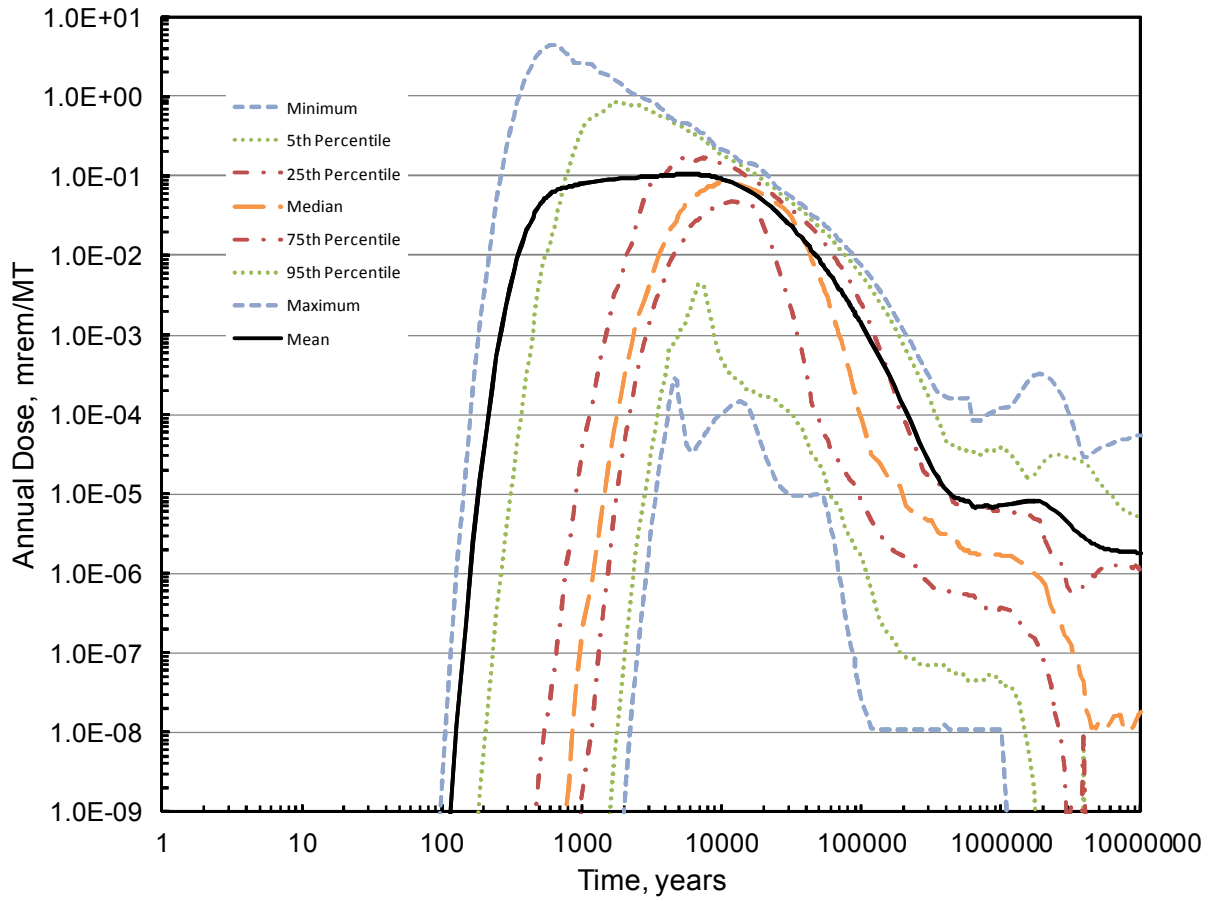
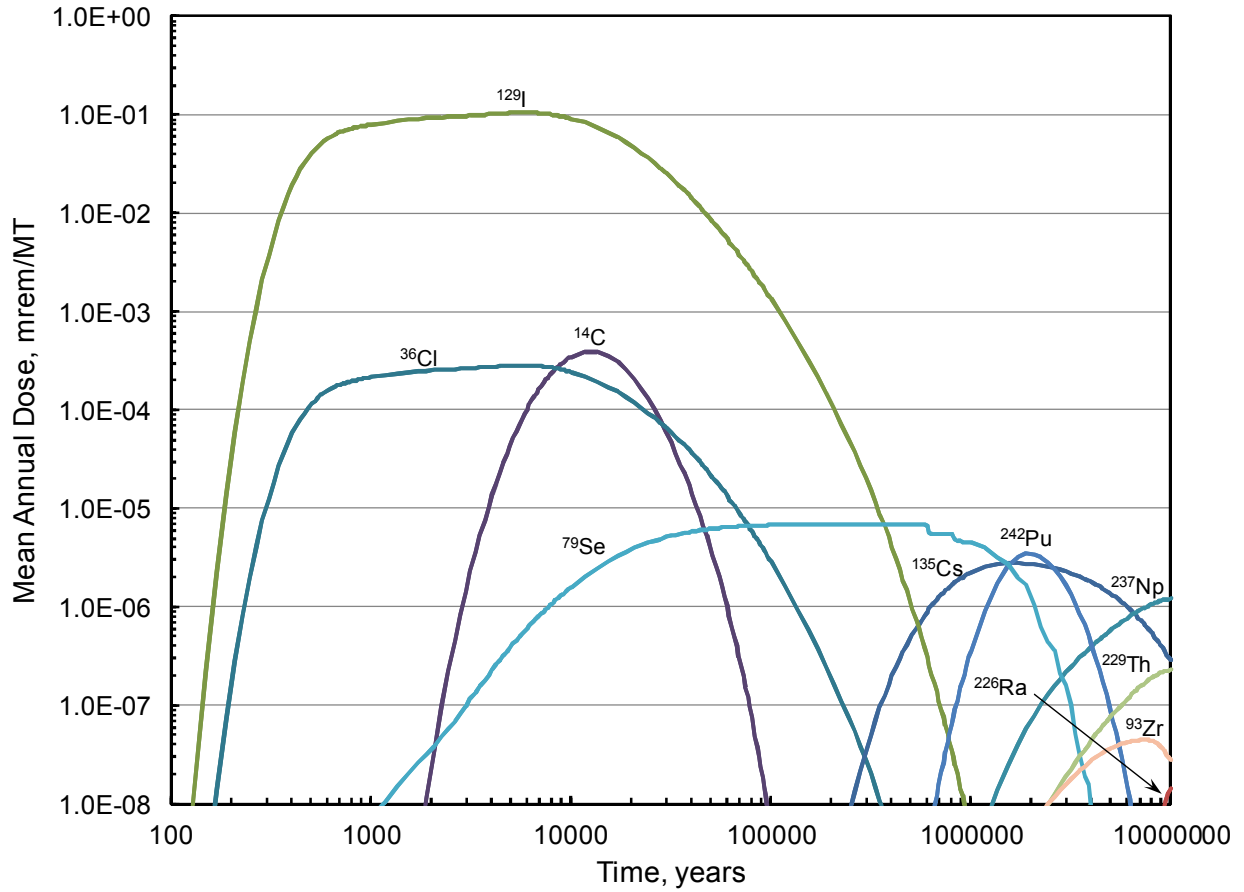Figure 21. Mean and Various Percentiles for the Annual Dose for a Fast Path that Intersects the Waste Form.

Figure 22. Major Isotopic Contributors to the Mean Annual Dose for a Fast Path that Intersects the Waste Form.
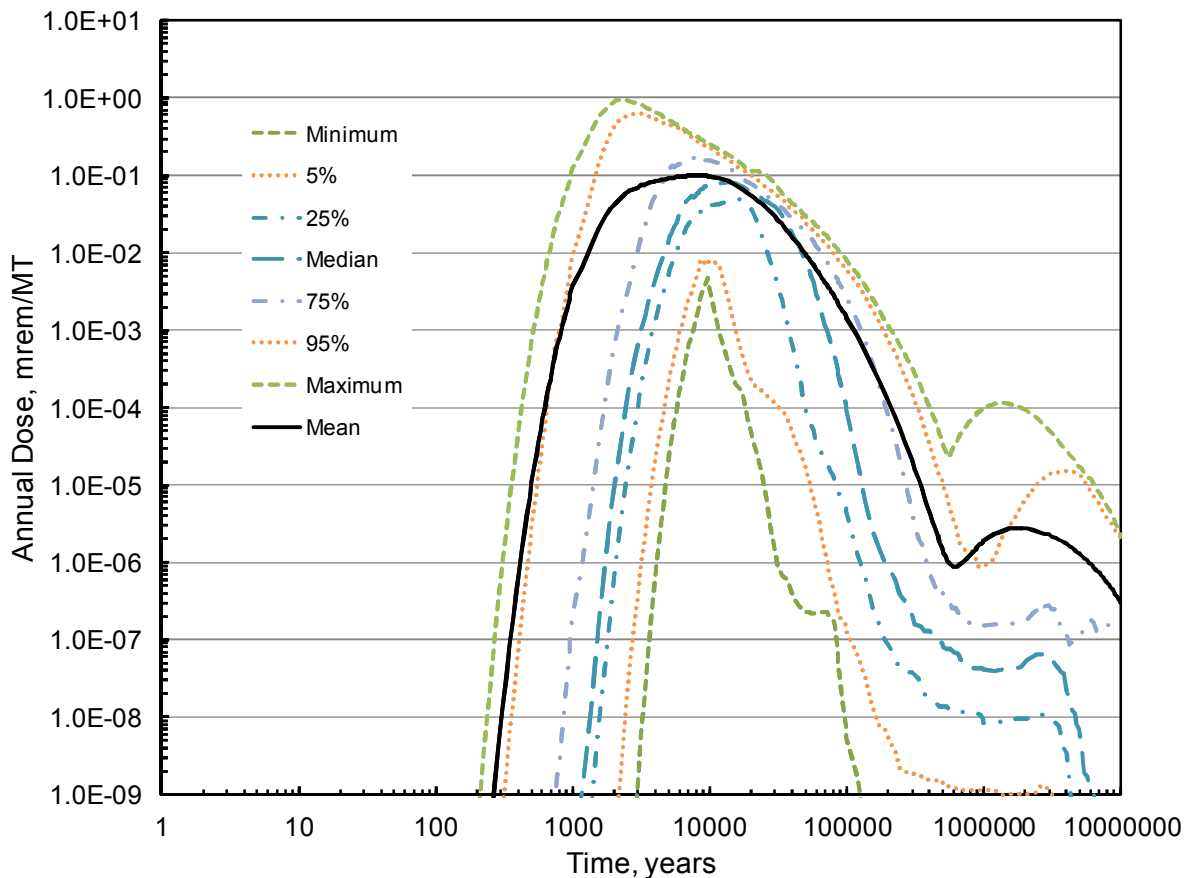
Figure 23. Annual Dose for Case with a 10-m Diffusive Path Between the Source and the Fast Pathway.

The fourth hypothetical fast pathway analysis further builds on the third case by requiring radionuclide transport through the degraded waste form, the primary engineered barrier, and secondary engineered barrier before entering the 10-meter diffusive pathway between the emplaced waste and the advective fast pathway. Just as in the reference cased described in Section 4.1 and unlike in the foregoing fast-pathway cases, the primary engineered barrier is postulated to remain intact for 10,000 years. Figure 24 shows the results for this case. The peak annual dose is about a factor of five lower that the results for the previous two fast-pathway cases but is nearly fifty times higher than shown for the mean annual dose shown in Figure 11 for the reference case. As in the previous cases, the mean dose is dominated by ^{129}I with ^{36}Cl and ^{135}Cs playing lesser roles. ^{242}Pu is the largest contributor among the actinides but its peak contribution is more than five orders of magnitude lower than the peak contributed by ^{129}I. As was the case for the results reported in Ref. 2, these results show that the characteristics of a hypothetical fast radionuclide transport pathway scenario and the associated properties can have a significant impact on the release of radionuclides from the hypothetical clay repository and particularly on the estimated annual dose.
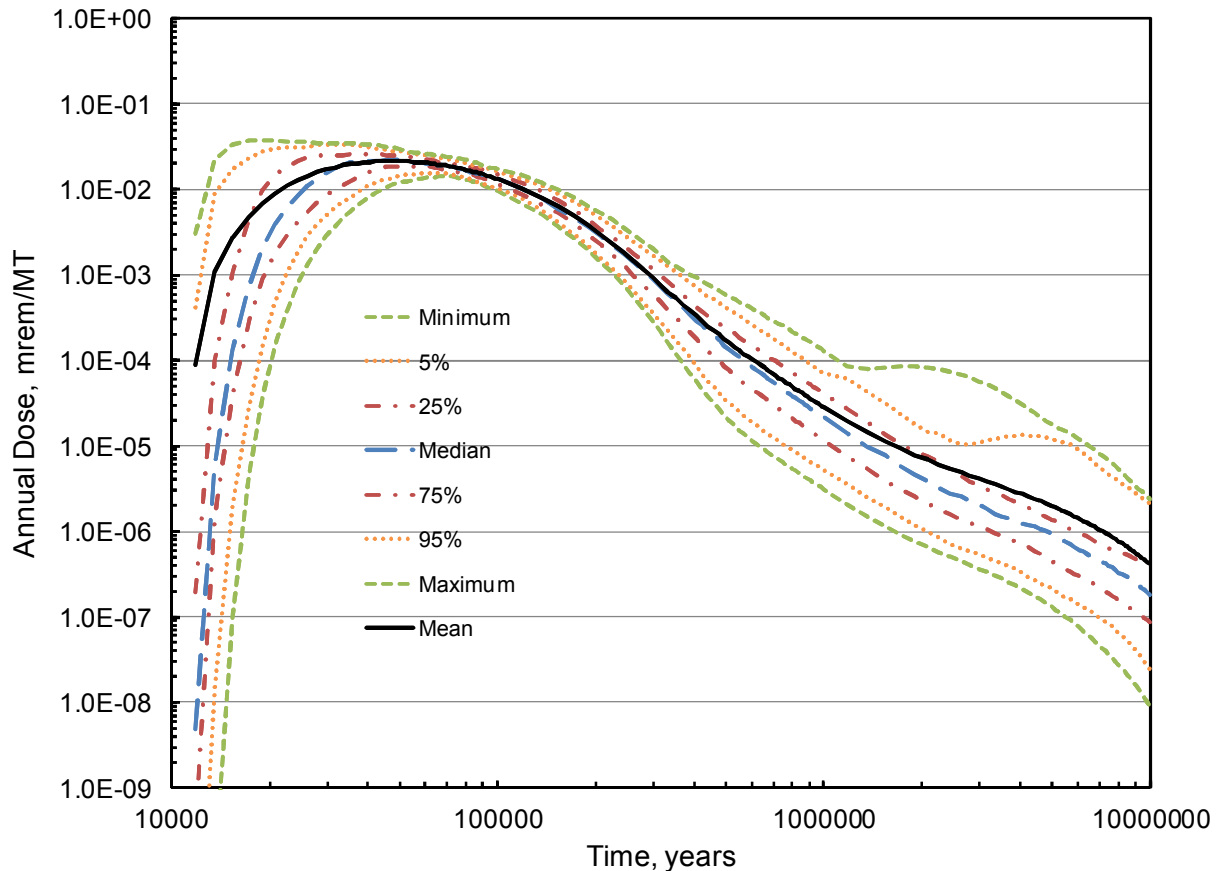
Figure 24. Annual Dose the Case of a 10-m Diffusive Path Between the Waste For and the Fast Pathway When the Engineered Barrier Functions as Designed.

5. CONCLUSION

The UFDC Clay GDSM described in Section 2 and in Ref. 2 has been applied to a hypothetical clay repository designed for the emplacement of waste packages containing 32 PWR spent fuel assemblies with burnups as high as 60 GWd/MT. Taking thermal considerations into account, the drift spacing in such a repository must be nearly a factor of eight larger than that considered in Ref. 2 where the waste packages contained only 4 PWR spent fuel assemblies. As might be expected, the annual dose, when normalized to a single metric ton of emplaced waste, is similar to that found in the earlier analysis.

For cases where a single fast path exists in the repository, the case when the fast path directly intersects the waste packages results in a peak mean annual dose significantly smaller than found in the analysis in Ref. 2 in spite of the larger waste package inventory. This is caused by the assumption that distribution coefficients for material in the fast path are the same as in the far field. These coefficients were assumed to be negligible in the previous analysis. For the cases where a diffusive path exists between the waste packages and the fast path or where both the diffusive path and a functioning engineered barrier exists, the peak mean annual dose was comparable to that found in the previous analysis. In these cases, both solubility limits and distribution coefficients in the diffusive path and in the engineered barrier system play a significant role in delaying the release of radionuclides to the biosphere. ,

6.   REFERENCES

1. F.D. Hansen, E.L. Hardin, R.P. Rechard, G.A. Freeze, D.C. Sassani, P.V. Brady, C.M. Stone, M.J. Martinez, J.F. Holland, T. Dewers, K.N. Gaither, S.R. Sobolik, and R.T. Cygan, "Shale Disposal of U.S. High-Level Radioactive Waste, " SAND2010-2843, May 2010.

2. D. Clayton, B. Freeze, T. Hadgu, E. Hardin, J. Lee, J. Prouty, R. Rogers, W. M. Nutt, J. Birkholzer, H. H. Liu, L. Zheng, and S. Chu, "Generic Disposal System Modeling – Fiscal Year 2011 Progress Report," FCRD-USED-2011-000184, August 2011.

3. A. Genty, G. Mathieu, and E. Weetjens, PAMINA: Performance Assessment Methodologies in Application to Guide the Development of the Safety Case, Final Report on Benchmark Calculations in Clay, Deliverable D-N°:4.2.4, October 10, 2009.

4. E. Weetjens, PAMINA: Performance Assessment Methodologies in Application to Guide the Development of the Safety Case, Report on First Results of Benchmark Calculations on Geometric Complexity (Clay Case), April 4, 20

5. ANDRA, Dossier 2005 Argile, Architecture and Management of a Geological Repository, 2005.

6. ANDRA, Dossier 2005 Argile, Phenomenological Evolution of a Geological Repository, 2005

7. ANDRA, Dossier 2005 Argile, Safety Evaluation of a Geological Repository, December 2005

8. W.M. Nutt, Y. Wang, J. Lee, "Generic Repository Concept Analyses to Support the Establishment of Waste Form Performance Requirements – Fiscal Year 2009 Year-End Status", ANL-AFCI-295, September, 2009.

9. GoldSim version 10.11, GoldSim Technology Group, 2010.

10. IAEA (International Atomic Energy Agency) 2003. Reference Biospheres for Solid Radioactive Waste Disposal. IAEA-BIOMASS-6. Vienna, Austria: International Atomic Energy Agency.

11. Sandia National Laboratories, Total System Performance Assessment Model/Analysis for the License Application, MDL-WIS-PA-000005 Rev 00, January 2008

12. Ernest Hardin, Teklu Hadgu, Dan Clayton, Rob Howard, Harris Greenberg, Jim Blink, Montu Sharma, Mark Sutton, Joe Carter, Mark Dupont, and Philip Rodwell, "Repository Reference Disposal Concepts and Thermal Load Management Analysis," FCRD-UFD-2012-000219 Rev. 2, November 2012.